Biosensors and Bioelectronics xx (xxxx) xxxx–xxxx

Contents lists available at ScienceDirect

Biosensors and Bioelectronics

journal homepage: www.elsevier.com/locate/bios

# Advances in digital polymerase chain reaction (dPCR) and its emerging biomedical applications

Lei Cao[a,b], Xingye Cui[a,b], Jie Hu[a,b], Zedong Li[a,b], Jane Ru Choi[a,b], Qingzhen Yang[a,b], Min Lin[a,b], Ying HuiLi [c], Feng Xu[a,b,*]

[a] The Key Laboratory of Biomedical Information Engineering of Ministry of Education, School of Life Science and Technology, Xi'an Jiaotong University, Xi'an 710049, PR China

[b] Bioinspired Engineering and Biomechanics Center (BEBC), Xi'an Jiaotong University, Xi'an 710049, PR China

[c] Foundation of State Key Laboratory of Space Medicine Fundamentals and Application, China Astronaut Research and Training Center, Beijing 100094, PR China

ARTICLE INFO

*Keywords:*
Deoxyribonucleic acid
Absolute quantification
Digital PCR
Droplet
Microwell
Microfluidics
Beads

ABSTRACT

Since the invention of polymerase chain reaction (PCR) in 1985, PCR has played a significant role in molecular diagnostics for genetic diseases, pathogens, oncogenes and forensic identification. In the past three decades, PCR has evolved from end-point PCR, through real-time PCR, to its current version, which is the absolute quantitive digital PCR (dPCR). In this review, we first discuss the principles of all key steps of dPCR, *i.e.*, sample dispersion, amplification, and quantification, covering commercialized apparatuses and other devices still under lab development. We highlight the advantages and disadvantages of different technologies based on these steps, and discuss the emerging biomedical applications of dPCR. Finally, we provide a glimpse of the existing challenges and future perspectives for dPCR.

## 1. Introduction

Nucleic acids, which include deoxyribonucleic acid (DNA) and ribonucleic acid (RNA) are among the most important biomacromolecules found in living organisms that carry genetic information, and thus have been used as an essential biomarker for detection of various diseases, such as infectious diseases (Chapman and Hill, 2012; Churchill et al., 2016; Deeks et al., 2012; Hofer, 2016), neoplasm diseases (de Magalhaes, 2013; Kanwal and Gupta, 2012; Schwarzenbach et al., 2011; Vogelstein et al., 2013), and cardiovascular diseases (Ball, 2013; Kathiresan and Srivastava, 2012; Konstantinidis and Kitsis, 2012; Lalani et al., 2013; Susiarjo and Bartolomei, 2014). In diagnosis of inherited or acquired disorders, nucleic acid testing is normally performed to determine the target concentrations (*e.g.*, copy numbers of target nucleotide sequences). However, the concentration of target nucleic acids in clinical samples, for example in blood, is typically low (*e.g.*, ~180 ng/mL (Allen et al., 2004; Schwarzenbach et al., 2008)), which is normally undetectable by most existing detection methods, hence necessitating the amplification process. Polymerase Chain Reaction (PCR) represents the most widely used nucleic acid amplification technology for amplifying and detecting the low concentration of nucleic acids. PCR is essential to make more copies of nucleic acids available for chemical identification (Kleppe et al., 1971). Since its invention in 1980s, PCR has found widespread applications in medical diagnosis, environmental monitoring (Ottesen et al., 2006; Tadmor et al., 2011) and food safety analysis (Burns et al., 2010; Chapela et al., 2015; Floren et al., 2015; Köppel and Bucher, 2015; Marcheggiani et al., 2015; Morisset et al., 2013). The first generation of PCR, termed end-point PCR, was developed in 1983 for target amplification, which however could only provide relative and qualitative results (Bartlett and Stirling, 2003; Saiki et al., 1985). Thereafter, the second generation of PCR, Real-time quantitative PCR (or qPCR), was developed in 1992 for target amplification and detection by using either fluorescence-based probes or dyes. Even though this technique enables quantitative detection, it is unable to provide absolute result (exact quantity of target), due to the issue of amplification bias that comes from fluorescence baseline estimation errors and polymerase's preference on amplification efficiency in qPCR (Ruijter et al., 2009; Tellinghuisen and Spiess, 2015b). In addition, this PCR technique is highly dependent on operator skills and relies on standard references, which requires a number of optimizations and validations (Schmittgen and Livak, 2008; Tellinghuisen and Spiess,

* Corresponding author at: The Key Laboratory of Biomedical Information Engineering of Ministry of Education, School of Life Science and Technology, Xi'an Jiaotong University, Xi'an 710049, PR China.
*E-mail address:* fengxu@mail.xjtu.edu.cn (F. Xu).

http://dx.doi.org/10.1016/j.bios.2016.09.082
Received 18 August 2016; Received in revised form 23 September 2016; Accepted 24 September 2016
Available online xxxx
0956-5663/ 

2015a). The standard internal references would differ from lab to lab and even may be inconsistent in duplicate experiments. However, standard dilution curves and reaction efficiency are not longer needed in digital PCR and it is this point that is one of the major issues in qPCR, especially at the lower limits of detection.

Recently, dPCR has been developed as a nucleic acid quantitative technique with unparalleled sensitivity (Huggett et al., 2013; Vogelstein and Kinzler, 1999), where a trace amount of nucleic acid is sufficient to obtain reliable quantitative results (Marx, 2014). The term “digital” represents the signal switching (*e.g.*, off or on, clotted or not clotted, activated or not, fluorescent or non-fluorescent) in single entities (Witters et al., 2014). In dPCR, DNA templates are initially diluted to a certain concentration (Majumdar et al., 2015) (*e.g.*, a few hundred to several thousand copies per microliter), which statistically results in one or zero molecule in reaction chambers prior to amplification. However, even under a sufficient dilution, the chances of more than one molecule per reaction are always there (especially statistically). Most dPCR instruments therefore adopt the Poisson distribution (Debski et al., 2015; Dong et al., 2015; Majumdar et al., 2015) and novel applications are suggesting negative binomial distributions as the Poisson distribution is only correct in a theoretical setting with now variation in partition sizes (Kreutz et al., 2011; Whale et al., 2012). Amplification products are generally detected by fluorescent probes and the chambers that contain a single template molecule yield positive signals. The exceptional cases with two or more targets would produce unusual fluorescence intensity that can be used to eliminate them. Thus the number of chambers with positive signal can provide a digital readout which allows absolute target quantification, avoiding the issue of amplification bias (Streets and Huang, 2014). Compared to conventional PCR technologies, dPCR enables a more precise, sensitive and reproducible target quantification. In dPCR, nucleic acid sample is partitioned into a mass of compartments (*e.g.*, droplets and microwells) or chambers, which are evaluated individually after amplification, hence the outcome is unaffected by the variations in the amplification efficiency. In addition, evaluation of an individual compartment in dPCR reduces the background signal by increasing the signal-to-noise ratio, thus significantly improving the detection sensitivity (Belmonte et al., 2016; Bhat and Emslie, 2016; Svobodova et al., 2015; Taylor et al., 2015).

Today, dPCR has attracted significant research interest, as reflected by the increasing number of publications (Fig. 1), which mainly focus on the concept or development of dPCR (Barrett and Chitty, 2014; Day et al., 2013; Huggett et al., 2013; Li et al., 2012; McCaughan and Dear, 2010; Zhang and Xing, 2010). Besides, there are limited reviews on the different existing dPCR commercial platforms (Baker, 2012; Marx, 2014; Perkel, 2014) However, the whole process, key steps, biomedical applications and perspectives of dPCR have not been systematically reviewed. In view of the rising need for highly sensitive, precise and accurate target quantification with the requirement for only a small amount of sample, there is a strong demand for a timely and comprehensive review on dPCR. In this review, we first discuss the principles of all key steps of dPCR, including sample dispersion, amplification, and quantification, applied to those commercialized apparatuses and other devices under lab development (Fig. 2). We highlight the advantages and disadvantages of different technologies based on these steps, and discuss the emerging biomedical applications of dPCR. Finally, we provide a glimpse of the existing challenges and future perspectives for dPCR.

## 2. Sample dispersion

Sample's dilution and dispersion is usually the first step in dPCR (Vogelstein and Kinzler, 1999). For a high throughput analysis (*e.g.*, thousands of reactions), the reaction volume for each compartment is normally reduced to nano/picoliter scale. In this case, the samples are separated into a large number of compartments for single molecule analysis, which could successfully increase the detection accuracy, and realize multiple target detection in a high-throughput manner. As a result, the most of DNA molecules could be fully dispersed in the separated compartments (*e.g.*, micro-chambers) containing “0” or “1” molecules (*i.e.,* negative or positive reaction) in each partition. Of course, few exceptional case with two or more targets would be identified by it's unusual fluorescence signal and the correct count is acquired. By creating individual reaction chambers, the cross-contamination between neighboring compartments could be avoided to achieve absolute quantification of targets in each sample.

For sample dispersion, there are four parameters that could significantly affect the dispersion results, *i.e.*, compartment size (*i.e.*, digitized sample volume), throughput capability (*i.e.*, number of compartments), reaction thermal stability, and dispersion rate (Baker, 2012; Day et al., 2013; Marx, 2014). Large compartment size could accommodate a large volume of sample that may contain more than one DNA molecule, making the result less reliable, while separating the equal sample into a smaller volume may acquire a large quantities of compartments that is beneficial to reaching a lower detection limit. In addition, the common compartment volume(range from hundreds of pico-liters to a few nano-liters) may not be able to hold some DNA molecule (*e.g.*, non-fragmented genomic DNA samples). In these cases, the DNA molecule have to be fragmented (Milbury et al., 2014; Nie et al., 2008). Nevertheless, the quantification preci-

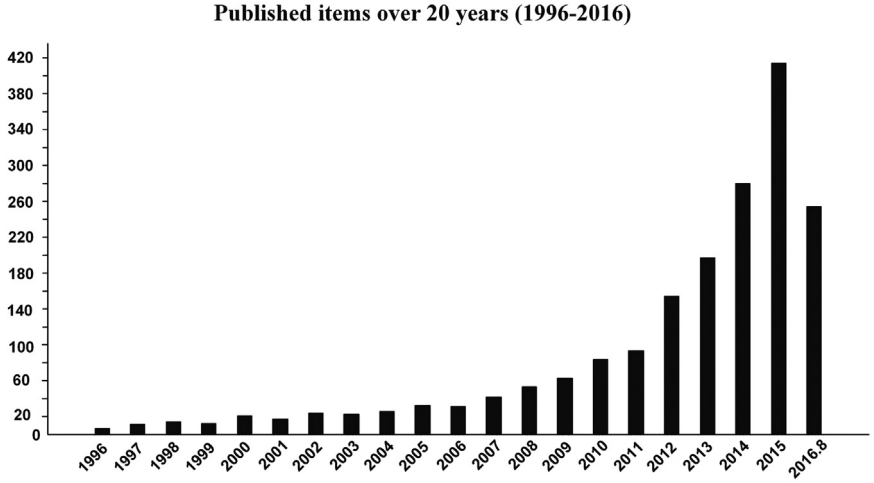


**Fig. 1. Digital PCR Publications from 1996 to 2016**. Data from web of science database. The following general search string was used: topic=(digital PCR) and published=1996–2016.8).

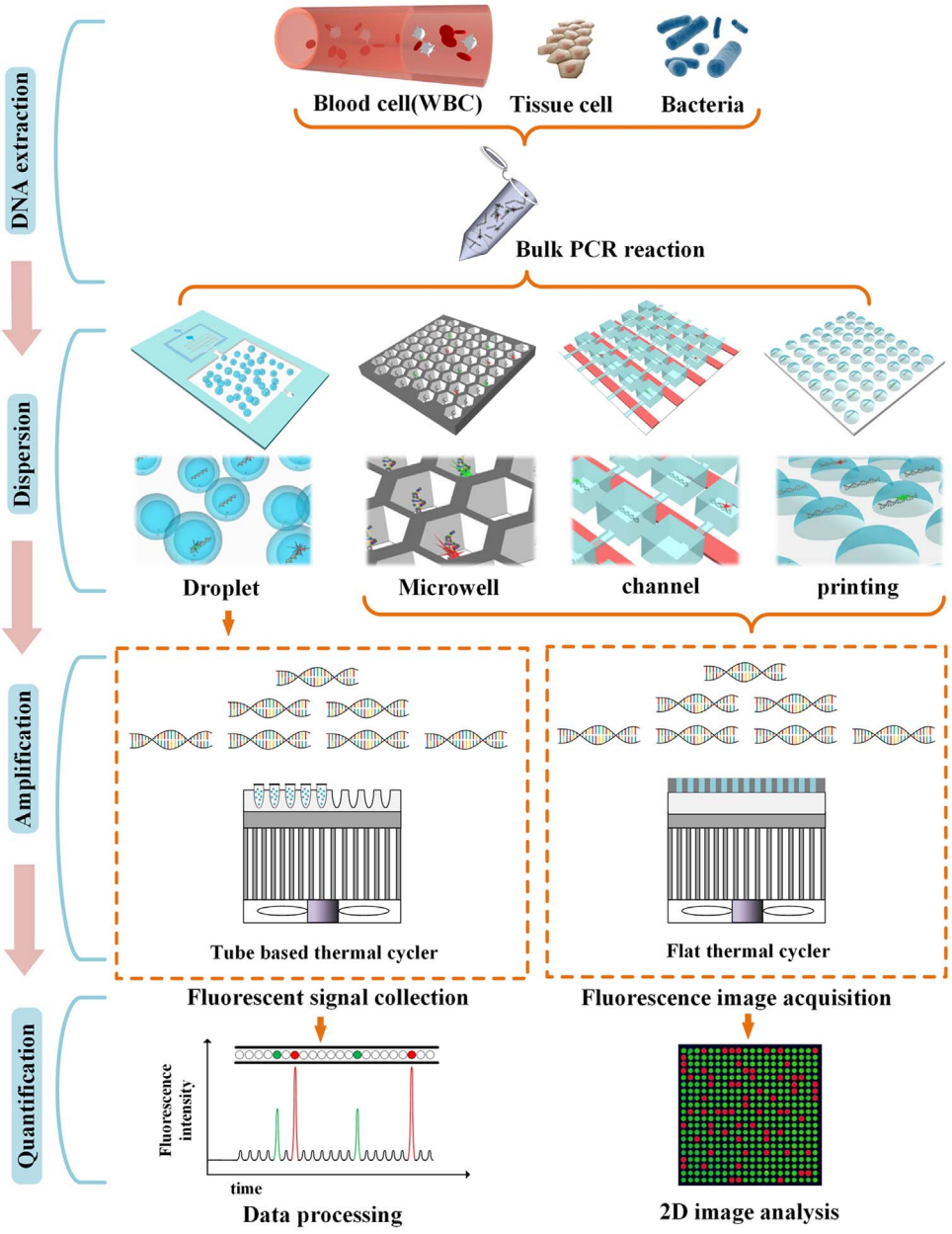


**Fig. 2. Principles in digital PCR**. There are mainly four ways for dispersing diluent nucleic acid molecules extracted from white blood cells, tissue cells or bacteria: droplet based sample dispersion, micowell based sample dispersion, channel based sample dispersion and printing based sample dispersion. Fluorescent signal collection of droplet method is applicable for photomultiplier tube (PMT) detection, and the other methods rely on CCD or complementary CMOS for capturing 2D fluorescent images.

sion, especially, mutation quantification could be confounded by heat-induced mutations during heat-induced fragmentation (Bhat et al., 2011; Kang et al., 2016; Knierim et al., 2011). As for the evaluation of throughput capability, dPCR reaction system that contains more compartments can accommodate more target molecules from sample, having a larger probability of detecting the target with extremely low concentration, and hence providing more sensitive and accurate quantification result. Besides compartment size and throughput capability, reaction thermal stability is also a key factor to be considered in sample dispersion. Reaction thermal stability is often defined as the percentage of compartments that are still readable after thermal cycling, which is inherently affected by evaporation rate and template loss. Sample evaporation and cross-contamination normally occur in thermal cycling that would reduce the efficiency of the assay. Besides, slow sample dispersion rate would directly increase the detection time, adding more complexity, thus hindering application of dPCR in point-of-care tests. In short, a dPCR system with small size of compartment, good thermal stability, high throughput, with high dispersion rate is highly desirable (Hudecova, 2015).

To date, various sample dispersion methods have been developed for dPCR including droplet-based sample dispersion, micowell-based-capillary force driving sample dispersion, channel-based sample dispersion, hydrogel bead based sample dispersion and printing based sample dispersion, *etc.* (Fig. 3). These methods are compared in terms of compartment size, compartment volume, partition number, reaction thermal stability and dispersion rate in Table 1. The advantages and disadvantages of these methods will be briefly discussed in the following sections..

### 2.1. Droplet-based sample dispersion

As the earliest and most widely used dPCR, droplet-based dPCR has made great achievements in many scientific fields (Beer et al., 2007; Guan et al., 2015; Hindson et al., 2011; Mazutis et al., 2009; Strain

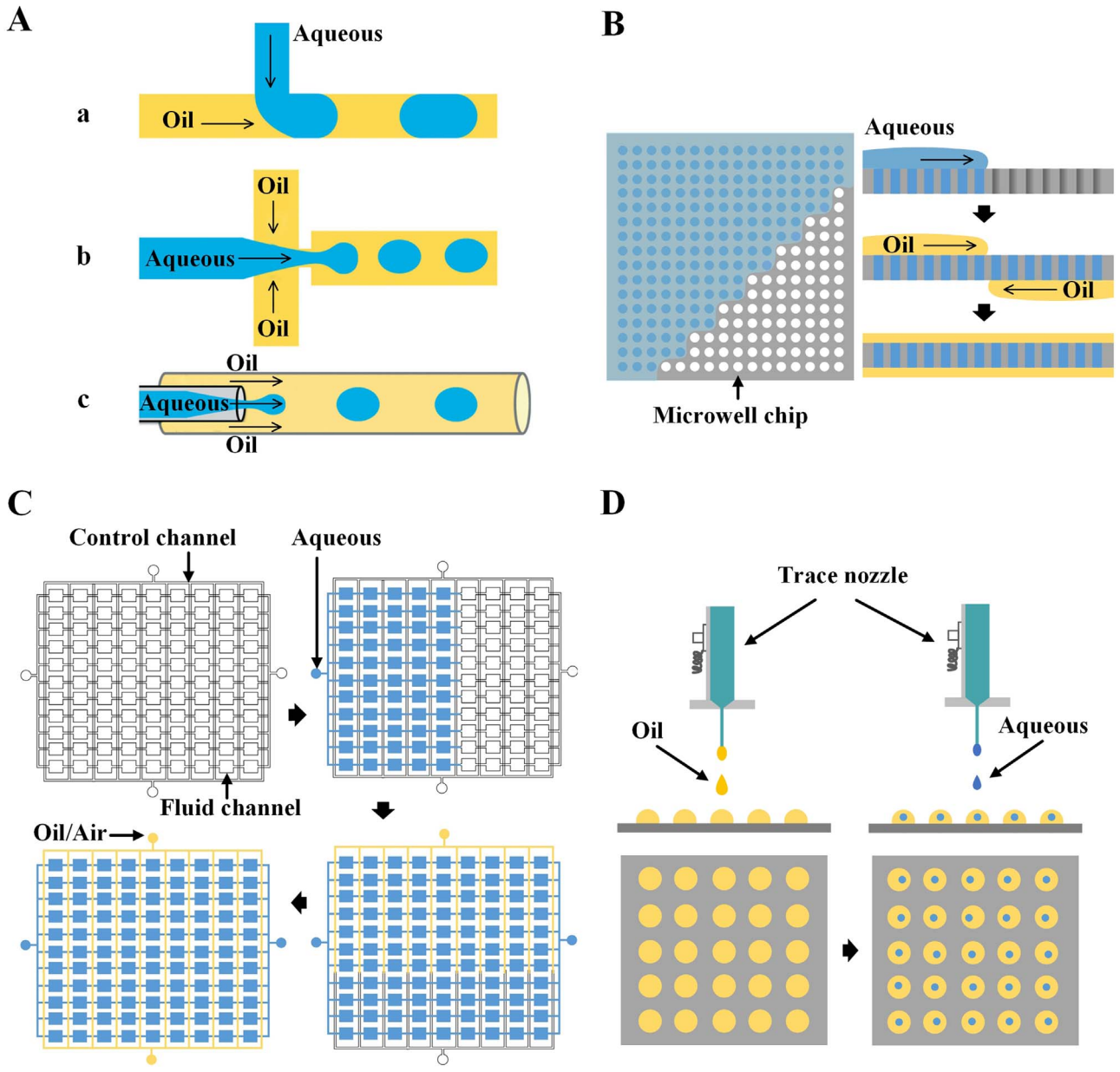


**Fig. 3. Schematics of different DNA sample dispersion methods**. **(A)** Droplet based sample dispersion (Shembekar et al., 2016; Zhong et al., 2011) or hydrogel bead based sample dispersion. There are mainly three design for generating water-in-oil droplets: (a) T-junction geometry (aqueous phase is sheared by oil and thereby generates droplets) (b) Flow-focusing geometry (droplets produced by shearing the aqueous stream from two directions) (c) Co-flow geometry (aqueous phase is ejected through a thin capillary, which is placed co-axially inside a bigger capillary, through which oil is pumped). **(B)** Micowell based sample dispersion. The hydrophilic modification of inner wall and the capillary force of these through-holes could keep the sample in place, producing nucleic acids' monomolecular dispersion on surface modified microwell chips. Sealing oil is injected onto both sides of the chip to preventing sample evaporation and cross-contamination during thermal cycling. **(C)** Channel based sample dispersion (Blow, 2007; Heyries et al., 2011; Ottesen et al., 2006). Channel based dPCR chip consists of two PDMS channel layers: fluid channel and control channel. After the fluid channel is filled with aqueous/nucleic acids sample, oil or air is pumped into control channel to produce the pressure to compartment fluid channels. **(D)** Printing based sample dispersion (Sun et al., 2014). The volume of each droplet printed on substrate is about 0.8 nl, and the quantity is 400 (20×20). Images reprinted from (Shembekar et al., 2016). (For interpretation of the references to color in this figure, the reader is referred to the web version of this article.)

et al., 2013; Tay et al., 2015; Wang et al., 2015). Droplet-based sample dispersion only requires a sample fluid volume in the micro- or nano-liter range to produce a large number of uniform droplets in oil phase *via* microemulsion, where thousands of parallel reactions can simultaneously happen (Fig. 3**A**). Water-in-oil droplets can normally be achieved by channel array on silicon, T-junction (Link et al., 2004; Nisisako et al., 2002) on acrylated urethane, polymethyl methacrylate (PMMA) and polydimethylsiloxane (PDMS), and shear-focusing on PDMS (Tanaka et al., 2015; Teh et al., 2008). In this process, a specific concentration of DNA and PCR mixtures (including Taq DNA polymerase, primers, TaqMan probes and dNTPs) are added into the microchannel. The PCR solution is emulsified in the microchannel of flow-focusing microfluidic chip, generating water-in-oil droplets with nanoliter volume for the following thermal cycling. Since molecular concentration is much less than the quantity of droplets, most of droplets contain either one or zero target molecule under the guidance of Poisson distribution. The PCR reaction is conducted on each droplet, and the droplets are collected for photomultiplier (PMT) or flow cytometry (FCM) analyzing (Bio-Rad, 2013). During amplification, only the droplets containing target DNA molecules will accumulate fluorescence as a result of TaqMan probe cleavage. The interpretation of a phosphor is "1", while opposite is "0", in which the threshold value is determined based on the fluorescence's Poisson distribution (Kreutz et al., 2011; Majumdar et al., 2015; Trypsteen et al., 2015). Finally, by

**Table 1**
Comparison of different DNA sample dispersion methods (Baker, 2012; Day et al., 2013).

| Sample dispersion method | Dispersion parameters | | | | |
|---|---|---|---|---|---|
| | Compartment size (m) (Streets and Huang, 2014) | Compartment volume | Throughput capability | Reaction thermal stability | Dispersion rate |
| **Droplets** | $10^{-4}$–$10^{-5}$ | 1 pL–1 nL | 20,000–10,000,000 | ** | ~2,000/min |
| **Microwell** | $10^{-5}$–$10^{-6}$ | 0.8–1.0 nL | 20,000 per chip each generate channel | **** | ~60,000/min |
| **Channels** | $10^{-4}$–$10^{-5}$ | 6.25 nL | 14,112 per sample panels | *** | ~10,000/min |
| **Beads** | $10^{-4}$–$10^{-5}$ | – | 10,000,000 | ** | ~3,000,000/min |
| **Printing** | $10^{-4}$ | 0.8 nL | 400 (each experiment) | *** | ~100/min |

counting the positive droplets' quantity, the concentration of target DNA in the sample could be determined.

In recent years, Bio-Rad® has developed and commercialized the QX100™ and QX200™ digital PCR systems. When performing the assay, 20 μl dPCR mix and DNA sample is loaded into an multichannel (8-channel), disposable droplets generation cartridge. Subsequently, 60 μl of mineral oil containing biocompatible surfactant and emulsion stabilizer is loaded into oil inlets. Thereafter, the cartridge is connected to a droplet generator. The generator produced a vacuum to the cartridge outlet, thus creating a negative pressure across the cartridge. Thereafter, the pressure drives and partitions the DNA sample stored in sample well into approximately 20,000 uniformly monodisperse water-in-oil droplets simultaneously (Hindson et al., 2013). In general, it can produce micro-droplets with an average volume of 1 nL or smaller. Recently, RainDance® has launched a water-in-oil based dPCR system (called Rain Drop™) with smaller sized compartments, which is capable of producing 100,000 microdroplets each with a 5 pL volume (Baker, 2012; Huggett et al., 2013).

Collectively, droplet-based dPCR (Dangla et al., 2013; Teh et al., 2008; Zhang and Xing, 2010) provides simple and accurate quantification of targets (Eastburn et al., 2013; Schneider et al., 2013; Zhang and Xing, 2010). This method ensures control of approximately uniform droplet size and droplet composition, and enables mixing, transferring and analyzing of each individual droplet. Secondly, due to the high specific surface area of micro-scaled droplets system, the heat transfer rate could be increased obviously, thus accelerating PCR reaction. In particular, producing droplets in oil phase could prevent potential cross-contamination among droplets and nonspecific amplification. However, because the liquid barrier among aqueous droplets is likely to break up during droplets transfer and thermal cycling at some times, confused results would appear at sometimes. In the future, the trends of droplet-based dPCR should be more sophisticated and multifunctional, especially in device design, optimization, fabrication and system integration.

### 2.2. Micowell based sample dispersion

The microwell based sample dispersion is an attractive alternative to the water-in-oil strategy, because it combines the parallelism of microarrays (Lindstrom and Andersson-Svahn, 2011) with the good quantification, high specificity and sensitivity of dPCR (Brenan and Morrison, 2005). The main step of this method is fabrication of a microwell array chip (most of case through holes). Initially, dense array of microscaled through-holes are built on the rigid chip (mostly on a silicon chip) (Fig. 3**B**). Then, physical or chemical methods are applied for surface modification (hydrophobic or hydrophilic surface). With the microwell array, it is possible to produce thousands of nanoliter microreactors in which single molecular amplification occurs. Highly specific polychromatic fluorescent-labeled oligonucleotide probes are adopted, thereby achieving sensitive and specific target quantification. Finally, a dedicated two-dimensional image acquisition device is used for image capture and analysis. The templates in microwell react specifically with labeled probes during PCR, producing signals that reveal the identity and concentration of each labeled target in the sample (Stears et al., 2003).

Microwell-based dPCR has been developed and commercialized in 2013 by Thermofisher®, offering a great market potential due to its convenience and reliability. One of the most representative microwell based dPCR chips is Quant Studio 20K™ chip (ThermoFisher, 2015). It consists of hydrophobic chip surface and wells with hydrophilic inner wall. The microwell silicon chip is generally fabricated by photolithography. It contains 20,000 hexagonal wells with a 0.8–1 nl volume. It is worth mentioning that they are all through-holes. In fact, the hydrophilic modification of inner wall and the capillary force of these through-holes could keep the sample in place. After dispersion, sealing oil is injected onto both sides of the chip immediately to avoid evaporation and cross-contamination during thermal cycling (Fig. 3**B**). Several studies have demonstrated the applications of microwell-based dPCR (Conte et al., 2015; Laig et al., 2015; Sefrioui et al., 2015; Wu et al., 2014). For instance, Dimov's group has made a microwell array (20 μm long, 20 μm wide and 50 μm deep) on silicon *via* standard photolithography. The multiplex single-cell RNA cytometry has been performed on the chip with 60,000 reaction chambers (Dimov et al., 2014). In another study, microwell-based sample dispersion has been demonstrated by coupling the microwell with paramagnetic beads (Witters et al., 2013), and the assay could detect the target with a concentration ranging from 10 aM to 90 fM.

Due to the presence of solid barrier between adjacent microreactions, microwell based sample dispersion avoids the risk of droplets breaking up, thus reducing the probability of false positive test results. Because microwell based sample dispersion only needs one step to disperse all the samples, producing uniform compartments and the process is time-saving. It also has advantages in physical partitions and dispersion speed compared to other dispersion strategies. Furthermore, the simple 2D fluorescence image capturing integrated with fluorescent dots image processing greatly reduces the analysis time to a few minutes. Taken together, integrating this method into sample-to-answer microfluidic chip holds great potential to achieve rapid and robust point-of-care testing (POCT) (Yager et al., 2006).

### 2.3. Channel-based sample dispersion

Soft-lithography has been increasingly used in many molecular biology research (Mujahid et al., 2013; Whitesides et al., 2001), due to its advantages in access to a variety of materials (Qin et al., 2010), mechanical and thermal stability (Mogi et al., 2014), replication accuracy and chemical resistance. It is convenient and time-saving to fabricate the nano/microfluidic devices with high resolution, high aspect ratios, and low surface roughness, such as array of nano-dots or well structures, nano/microchannels, and other micro-structures (Blow, 2009; deMello, 2006; Sackmann et al., 2014; Velve-Casquillas et al., 2010). Recently, soft-lithography based multilayer-channels (Psaltis et al., 2006) and dPCR have been combined to create an innovative microfluidic chip called "microfluidic valve", which looks

similar to the integrated circuit transistor (Heyries et al., 2011; Tian et al., 2015a) and therefore is referred to "integrated fluid circuit (IFC)". Monolithic fabrication of the chip could be accomplished by multilayer soft lithography (Streets and Huang, 2014; Unger et al., 2000).

Briefly, PCR premix is initially mixed with the diluted DNA sample, and then transferred into a piece of PDMS microfluidics chip. Sample channel is composed of thousands of nano-fabricated small chambers connected in series. A certain amount of sample solution is added into the chambers, where DNA molecules are uniformly dispersed into these units, eventually forming a PCR reactions array that contains single nucleic acid molecule (*i.e.*, reaction layer). These small chambers are separated by "microfluidic valve". Another piece of PDMS film is used to divide the vertical channel of reaction layer. Micro-reaction chambers completely independent with each other are ultimately formed, and PCR reactions are carried out in a number of mutually independent small chambers (Blow, 2007; Nixon et al., 2014; Ottesen et al., 2006; Ramakrishnan et al., 2013).

The Fluidigm® has made significant achievements on the development of channel-based dPCR chip (termed IFC) (Ramakrishnan et al., 2013). Each microfluidic chip employ micromechanical valves (NanoFlex™ valve) to partition tens of microliters PCR mixture into 1176 independent reaction chambers (NanoFlex™ chamber, each is 6.25-nl) randomly (Ottesen et al., 2006). Once hydraulic or pneumatic pressure is applied to the control channel network (lower), the thin PDMS membranes between the control channels and fluid channels are deformed and deflected upward. This creates the so-called micromechanical valves. When these valves are closed under pressure, the continuous fluid network preloaded PCR mixture is partitioned into thousands of independent PCR microreactors (Fig. 3**C**).

Besides the IFC, other similar channel-based dPCR have also been demonstrated. For instance, Tian et al. (2015a) have designed and fabricated a multilayer PCR chip which is capable of performing DNA purification and dPCR detection. With the magnetic beads and external magnetic field, the steps of washing and elution of DNA are performed. DNA and PCR mix are introduced into reaction layer with individual chambers by the temporary negative pressure offered by suction layer, then, the main channels are filled with injected silicone oil to rushed away excess aqueous samples (Song et al., 2015). Another layer of PDMS is added, which is filled with water to keep the wettability of PCR reaction layer, reducing the evaporation of solvents. Similar to the multilayer chip design, a negative pressure driven dPCR chip made up of PDMS has also been developed with 650 chambers on the chip and 6.28 nl of sample in each chamber (Tian et al., 2015b). Another microfluidic device integrating cell capture, cell lysis, RNA reverse transcription and digital PCR is fabricated for single cell analysing (White et al., 2013). The difference from previous mentioned "IFC" is that it doesnot need pressure actuated control layer, but flowing oil to produce individual aqueous compartments. With this platform, three lung cancer related genes have been successfully quantified, suggesting the feasibility and flexibility of the chip for single nucleic acid molecule's amplification (Zhu et al., 2014).

In addition, a microfluidic device called "SlipChip" has been fabricated to accurately quantify nucleic acid in combination with PCR (Shen et al., 2010a, 2010b). The fluidic channel is assembled by independent wells in two glass plates. And when the two plates are aligned, wells in a line are connected one by one to become a fluent channel which introduces the sample and PCR mixture into the chip. Afterwards, the fluidic channel is broken up and restored to individual wells just by a single step of slipping the two plates. In this way, the overlaps among wells are removed and the aqueous sample in each well in contact with a reservoir preloaded with oil to generate hundreds of separate compartments simultaneously. In this work, the sample has been separated into 1280 chambers with 2.6 nl of each sample for single molecule detection. What's more, the unique "slip-break up" partitioning concept has been further optimized for a large and tunable dynamic range, *i.e.*, multivolume digital RT-PCR (MV digital RT-PCR) (Shen et al., 2011).

In short, employing the active partitioning strategy instead of dilution, channel-based sample dispersion is better than the other methods mentioned above in terms of sample loading, partition accuracy and reproducibility. However, the requirement for functional integration makes it much harder in design and fabrication process. In addition, the air permeability of PDMS film used in microfluidics may lead to risk of sample evaporation, even cross-contamination. And it's not an easy work to prison drops of PCR mix solution in chambers under thermal cycling.

### 2.4. Hydrogel bead based sample dispersion

Besides the water-in-oil droplet-based dPCR, other hydrogel bead based sample dispersion methods have also been introduced. For instance, multiplexed hydrogel bead based digital PCR (Qi et al., 2011) has been demonstrated using hydrogel microbeads and emulsification to produce micro-droplets containing template strands. Briefly, it includes three steps, *i.e.*, template preparation using common sequence labeled primers for reverse transcription, single molecule amplification based on microemulsion (Williams et al., 2006), and bead counting on a hydrogel-bead array. Moreover, it can detect multiple targets on a hydrogel-bead array. Detection limit of the assay can be as low as 0.1% (*i.e.*, a target molecule is detected from 1000 molecules). Using β-actin gene as a target analyte, the assay has been shown to achieve a detection limit as low as 100 cells.

Agarose beads based digital PCR can reduce cross contamination between droplets by transition into solidified agarose beads. This method has been used for single copy genetic analysis (Leng et al., 2010). In this assay, PCR mixture is dispersed to small droplets with the droplet size of 80–100 μm in oil phase when passing through the microfluidic channels. Droplet surface is uniformly wrapped by agarose gel. This "sol-gel switching" mechanism is capable of preventing cross-contamination between PCR droplets. Also, it makes the manipulation and preservation of droplets more convenient as for the temperature dependent phase transformation. Compared to the conventional "cloning-sequencing-chemical synthesis-screening" work flow for aptamer screening, agarose bead based digital PCR avoids large-scale sequencing and time-consuming synthesis of massive DNA aptamer candidates, providing a high screening efficiency (Zhang et al., 2012). Unlike fluid droplets, hydrogel (such as agarose) beads can be processed much easier and thus benefit for relevant downstream biomedical applications such as sequencing validation. Because of the low-cost "sol-gel switching" beads provide a natural partition strategy for DNA samples, there is no need for expensive micro-nano chip fabrication.

### 2.5. Printing based sample dispersion

Inkjet printing (Arrabito et al., 2013) has flexibility and high-throughput capability in the evolution of dPCR, which offers significant competitive advantages (Hoffmann et al., 2012). Combining droplet printing and dPCR, namely "printing-based dPCR", is capable of producing a customized instrument, which fits various experimental demands in the studies. Droplet printing-based dPCR typically involves a few operation steps (Fig. 3**D**), *i.e.*, oil droplet array is first printed on a hydrophilic-in-hydrophobic-patterned chemically modified substrate (Sakakihara et al., 2010; Zhang et al., 2011) and then sample micro droplets containing target nucleic acid and PCR mixture is printed into each oil droplet. And then, PCR thermal cycling reaction is performed and fluorescence dot images are acquired and analyzed at the end of reaction (Guttenberg et al., 2005; Sun et al., 2014). Inspired by droplet printing, it has been reported that hundreds of droplets have been printed on a hydrophobic and oleophobic surface to perform qPCR detection (Sun et al., 2014; Zhu et al., 2015). The droplet could reach the volume as low as 800 pL, which is encapsulated in a silicone oil

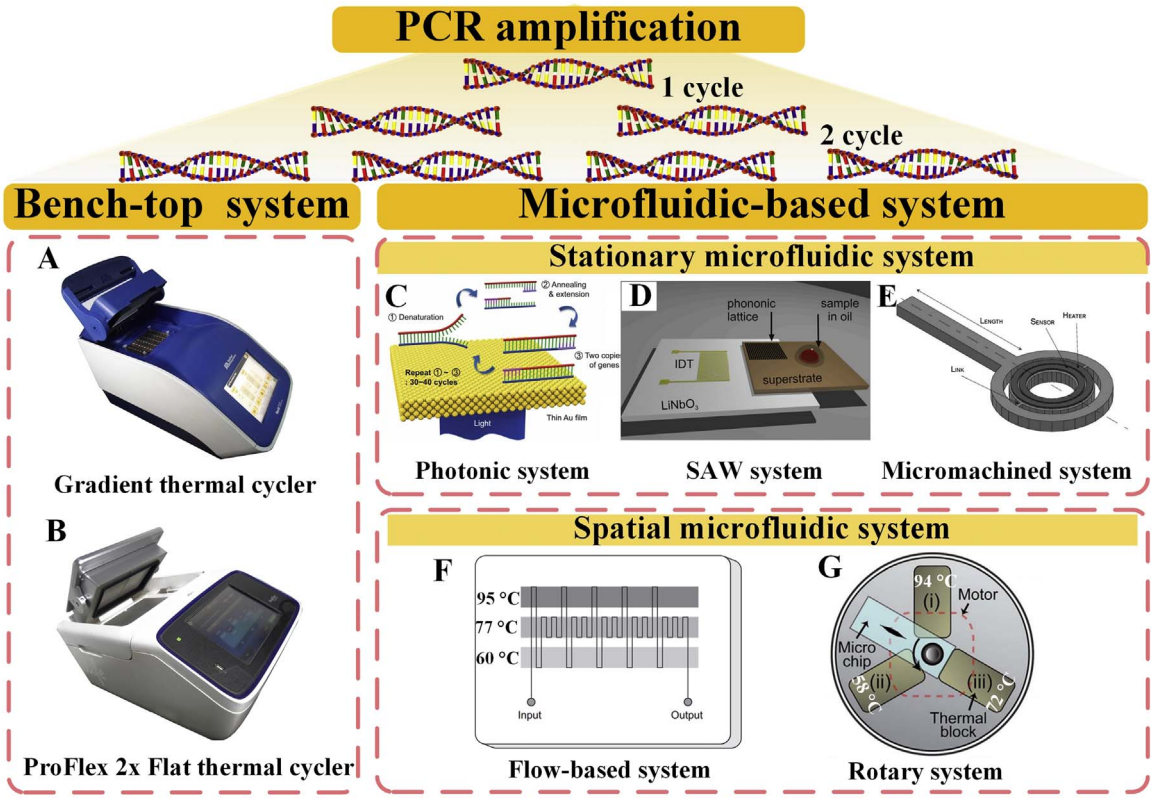


**Fig. 4. The thermal cycling systems for PCR amplification process including bench-top system and microfluidic-based system**. **(A)** Photograph of a gradient thermal cycler. **(B)** Photograph of a ProFlex™ 2x Flat PCR thermal cycler. **(C)** Schematic of the photonic system using a thin gold film as a light-to-heat converter and excitation light from the LEDs. **(D)** Setup of the SAW system. **(E)** Schematic of the micro machined system containing both the heater and sensor made of a thin film of metal and thermally connected by placing them at the same silicon ring. **(F)** Schematic of a flow-based system containing three individual thermostatic zones for PCR amplification. **(G)** Schematic illustration of a rotary system consisting of a microchip, three heat blocks, and a stepper motor. Images reprinted from (Jung et al., 2012; Kopp et al., 1998; Neuzil et al., 2006; Reboud et al., 2012; Son et al., 2015).

droplet, to avoid sample evaporation and cross-contamination during thermal cycling.

Taken together, with advances in droplet printing technologies, the droplet printing based dPCR offers great advantages in applicability, reproducibility and cost-effectiveness. Because of printing's customizability, the printed droplet size can be optionally changed to meet a variety of requirements during experiment (Li et al., 2015). The success in development of inkjet printing (Rose, 2000) or contact printing (Kim et al., 2009) technologies offers great potential to achieve single molecule DNA printing in dPCR in the near future.

## 3. Amplification process

Following the sample dispersion process, PCR amplification process is performed relying on repeated thermal cycling to the sample, commonly consisting of two or three distinct temperature stages for denaturation, annealing and extension. Conventional bench-top PCR thermal cyclers complete the process by heating and cooling the sealed tubes loaded with PCR reagent, which are mostly based on Peltier thermoelectric units functioning as both the heating and cooling elements (Fig. 4**A and B**). However, the amplification process is time consuming due to the relatively low temperature change rates 1.5–5 °C $s^{-1}$). In addition, these thermal cyclers are bulky, high cost, and high power consumption, hindering their extensive applications (Miralles et al., 2013). To address this, various new thermal cyclers have been developed recently for PCR amplification, showing attractive features of compact size, improved heating/cooling rates and reduced amplification time (El-Ali et al., 2004; Liao et al., 2005; Poser et al., 1997; Yoon et al., 2002). All these cycling systems can be classified into two systems based on the position between the sample and the thermal block during amplification, *i.e.*, stationary system and spatial system.

### 3.1. Stationary system

Stationary system is defined according to the position between the sample and the thermal block, in which no movement occurs during the PCR amplification process. Recently, various heating techniques have been integrated into microfluidic systems for PCR thermal cycling, including photonic heat- (Roche et al., 2012; Son et al., 2015), acoustic waves- (Shilton et al., 2015), and micro machined Joule heat-based system (Liao et al., 2005; Neuzil et al., 2006). Recently, to achieve photonic heating, laser-activated nanoparticles in solution have been demonstrated to be capable of heating the surrounding solution through the mechanism of light-to-heat conversion (Jaque et al., 2014). In addition, a thermocycler based on photonic heating has been proposed for PCR amplification. For example, gold nanoparticles with 60 nm diameter were activated by a 532 nm laser beam for heating and a fan was used for cooling, providing heating rate of 7.62 °C $s^{-1}$ and cooling rate of 3.33 °C $s^{-1}$ (Roche et al., 2012). However, this strategy is subjected to the high cost of the laser. More recently, an ultrafast photonic PCR thermal cycler based on using a thin gold film excited by light-emitting diodes for heating has been developed (Fig. 4**C**) (Son et al., 2015). Due to the high thermal conductivity of the gold film, the ultrafast heating (12.79 °C $s^{-1}$) was achieved by the light illuminated gold film with highly efficient light-to-heat conversion and fast cooling (6.6 °C $s^{-1}$) was obtained through the high thermal dissipation with the aid of a cooling fan. This method is characterized by low cost and low power consumption with ultrafast thermal cycling capability, without the need for expensive laser source, thus showing promising prospect for POCT.

Besides photonic heat-based system, acoustic waves-based system has also been introduced for thermal cycling. Acoustic waves have been widely applied to manipulate droplets on microfluidic chip owing to the

pressure wave within the droplet generated by acoustic energy (Friend and Yeo, 2011). The acoustic waves can also induce thermal effect when the acoustic energy is dissipated into the fluid (Kondoh et al., 2009). Reboud et al. (2012) have demonstrated that PCR amplification in a microliter droplet covered by oil using a thermocycler based on surface acoustic wave (SAW), where SAW was generated by the interdigitated transducer (IDT) and coupled into a disposable superstrate as an alternative to expensive SAW chip (Fig. 4**D**). In the configuration, the heating process was achieved by changing the input frequency and excitation power and the cooling process was achieved by passive thermal dissipation through a heat sink. Recently, a direct SAW actuated digital microfluidic heating strategy has been demonstrated with the SAW decoupled from other heating sources (Shilton et al., 2015). The experiment showed that the higher temperature change can be obtained with higher viscosity fluids (~10 °C for water), achieving rapid thermal cycling between 65.0 °C and 95.8 °C of a viscous glycerol droplet. The acoustic thermal cycling system is simple, easy to achieve and also easily integrated into a hand-held system.

Micro machined Joule heat-based system has also been reported. For example, Neuzil et al. have reported an ultrafast miniaturized PCR thermal cycling system, which enables the temperature ramp rates up to 175 °C $s^{-1}$ for heating and 125 °C $s^{-1}$ for cooling, respectively (Liao et al., 2005; Neuzil et al., 2006). In the system, both the heater and the sensor are fabricated by a thin film of Au/Cr metal deposited on the same micro machined silicon ring (Fig. 4**E**). Further, the miniaturized system has been integrated into handheld PCR instruments for rapidly detecting infectious diseases (Ahrberg et al., 2016a; Neuzil et al., 2010). However, the system is subjected to the high cost and complicated fabrication due to the need for e-beam evaporation, etching and lithographic process.

### 3.2. Spatial system

In the spatial microfluidic system, the PCR thermal cycling is completed through the position change between the sample and the individual thermostatical temperature blocks. For instance, Martin et al. have successfully demonstrated a continuous flow PCR on a glass chip, where the PCR sample was pumped sequentially and repetitively flowing through three individual thermostatic zones (Fig. 4**F**) (Kopp et al., 1998). Recently, a real-time quantitative PCR in picoliter water-in-oil droplets has been accomplished on a continuous flow-based thermal cycling, which enables quantification of target in each picoliter droplet, showing great prospect for dPCR application (Kiss et al., 2008). The amplification speed is fast due to the high speed of the flow rate and the cross-contamination could be avoided because of the spatially separated amplification cycles. However, in this configuration, the number of PCR amplification cycles was determined by the layout of the microfluidic channel on the chip. More recently, another liquid flow-based PCR relying on the pre-heated liquids heating the PCR chamber has been developed (Houssin et al., 2016). This strategy showed ultrafast temperature change rate with the maximum heating and cooling ramp rates of 25 °C $s^{-1}$ and 18 °C $s^{-1}$, respectively. Moreover, this system is compatible with large-volume samples (tens of microliters) with ultrafast temperature cycling rates and good temperature homogeneity, which shows higher sensitivity than that of low-volume samples due to the relatively low numbers of DNA templates in low-concentration samples. However, this system needs a reservoir and a heat exchanger for each heat-transfer liquid and a pressure controller for precisely controlling the liquid flow, thus making the system bulky and complicated.

Similar to the principle of flow-based PCR, rotary PCR systems have also been developed, in which the thermal cycling is performed through sequential rotation of the microchip containing PCR sample on three adjacent thermal blocks to accomplish the amplification process (Fig. 4**G**) (Jung et al., 2012). This system is fast and does not require precise control of liquid flow. Further, the cycling ramp rates of the rotary PCR could be dramatically improved by maximizing the thermal contact between the sample reactor and the thermal block. For instance, a capillary containing the sample was fixed in a recessed groove on the surface of the thermal block to minimize the thermal contact resistance, showing the maximum ramp rate of 44 °C $s^{-1}$ (Bartsch et al., 2015).

As stated above, various thermal cycling systems have been developed for microfluidic and droplet-based PCR application. Compared to bench-top systems, these systems are characterized by minimal size, low power consumption, low cost, easy operation and fast/ultrafast temperature change rates. Hence, these systems are well suited for dPCR amplification through the limiting dilution of sample on the microfluidic chip. However, the spatial systems are subjected to the precise control of the liquid flow and/or the friction wear during the rotation of the thermal block against the sample reactor, which could potentially be an issue for the long-term reliability of the system. On the other hand, the stationary systems require the heating/cooling elements to accomplish thermal cycling, which consume more power. In addition, microwave dielectric heating of the water-in-oil droplets shows great potential application for droplet-based PCR amplification, holding the ability to increase the temperature of drops rapidly (Issadore et al., 2009).

## 4. Quantification process

Depending on the sample dispersion strategies, the quantification processes in dPCR mainly rely on two methods (Fig. 5**A and D**). One is droplet-based fluorescence signal counting, determining the number of droplets that have different fluorescence intensity *via* the photomultiplier tube (PMT) (Mazutis et al., 2009, 2013), which is similar to the principle of flow cytometry. The other is chip-based fluorescent dots image processing, using the charge-coupled device (CCD) or complementary metal-oxide-semiconductors (CMOS), acquiring and analyzing the two-dimensional (2D) fluorescence bitmap images. Both quantification methods are integrated optical detecting systems with high precision, excellent sensitivity and resolution. The evaluation of different image processing techniques and principles used corresponding to different sample dispersion methods is summarized in Table 2. In dPCR quantification, an ideal fluorescent processing system must have high resolution, rapid detection, false positive screening, and high versatility (Lievens et al., 2016).

### 4.1. Droplet based fluorescence signal counting

Droplet-based fluorescence signal counting has been widely used in commercial dPCR instruments (QX100™ and QX200™, Bio-Rad®; Rain Drop™, RainDance®) (Baker, 2012; Chen et al., 2013; Day et al., 2013). After the amplification reaction in water-in-oil based dPCR, all of the droplets are collected in a custom transfer vial which is connected to the readout chip in a droplet reader. The oil is continuously introduced to the intersection under a constant pressure, aqueous droplets are then individually separated by the spacer fluid and being transferred to the subsequent laser-induced two-color detector (*i.e.*, the PMT) one by one at the rate of ~1000 per second (Pekin et al., 2011; Zhong et al., 2011) (Fig. 5**A and B**).

TaqMan assay has been performed for the duplex detection of target and reference genes using the dual fluorophores: Fluorescein amidite (FAM) and Aequorea victoria (VIC). Resulting from quenching failure of fluorescent probes during PCR, each droplet is bound to have an intrinsic fluorescence value. All of the droplets are gated by fluorescence peak width to filter out rare abnormal droplets (Pekin et al., 2011; Trypsteen et al., 2015; Zhong et al., 2011) (*e.g.*, doublets, triplets) (Fig. 5**C**). The data is recorded by imaging software, QuantaSoft™ analysis software (Bio-Rad®), based on the fluorescence amplitude using the droplet reader (Hindson et al., 2011). For the number of all droplets is known, proportion of positive (containing

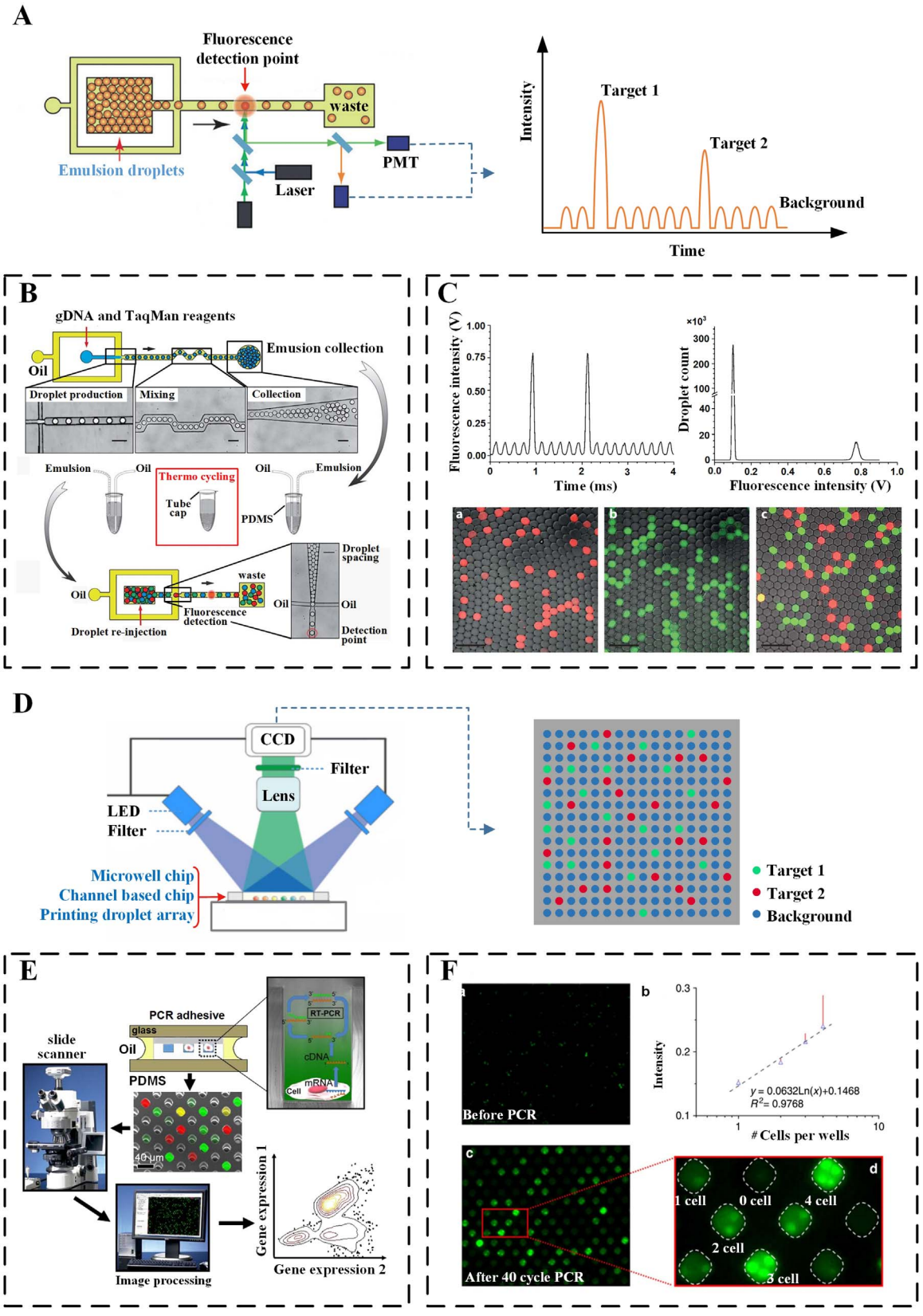


**Fig. 5. Quantification methods and representative results for dPCR. (A)** Droplet based fluorescence signal counting. As similar with a flow cytometry, Amplified droplets flowing through the dual-color fluorescence detection channel in sequence. For a single droplet containing Target 1 (modified by FAM™), Target 2 (modified by VIC™) or no templates, lasers with different excitation wavelength (494 nm and 538 nm) can produce the corresponding emitted light (518 nm and 554 nm), which is recorded by PMT1 and PMT2. Then, counting the number of characteristic peaks to get targets' proportions. **(B)** Quantitative and sensitive detection of rare mutations using droplet-based microfluidics (Pekin et al., 2011) (scale bar 60 μm). **(C)** Droplet readout by fluorescence value. Fluorescence is accumulated during PCR and each discrete burst of fluorescence corresponded to an individual droplet. Two groups of droplets were evident: PCR (+) droplets peaking at 0.8 V and PCR (-) droplets at 0.1 V (scale bar 100 μm) (Pekin et al., 2011; Zhong et al., 2011). **(D)** The other one is chip based fluorescent dots image processing, using the CCD, acquiring and analyzing the 2D fluorescence bitmap images. **(E)** Schematic of the process for discovering heterogeneity within

**Table 2**
Comparison of detection parameters of different dispersion methods (Baker, 2012).

| Sample dispersion method/ Detection principle | Sensitivity (Day et al., 2013) | False positive | Portability | Speed |
|---|---|---|---|---|
| Droplets/PMT or FCM | 0.000–0.01% | **** | ** | * |
| Microwell/CCD or CMOS | 0.005% | * | *** | **** |
| Channels/CCD or CMOS | 0.01% | *** | **** | *** |
| Beads/Scanner | 1% | ** | ** | ** |
| Printing/Scanner | – | ** | * | ** |

Notes: PMT: Photomultiplier tube, FCM: Flow cytometry, CCD: Charge-coupled device, CMOS: Complementary metal-oxide-semiconductors.

targets ) droplets is obtained to calculate the absolute concentration of target.

### 4.2. Chip based fluorescent dots image processing

Chip-based fluorescent dots image processing (Fig. 5**D**) includes acquisition of fluorescence image, image processing, and data analysis. With similar "2D fluorescent image capturing" process, microwell chip, channel based chip, hydrogel beads array and printing droplet array are applicable with the fluorescent dot imaging system (Zhu et al., 2015). Several fluorescent dots imaging approaches have been applied in dPCR (Dimov et al., 2014; Fan and Quake, 2007; Zhang et al., 2012; Zhong et al., 2011; Zhu et al., 2014), where selecting an appropriate imaging approach is essential to achieve an optimum result.

To achieve high resolution and quality fluorescence images of the dPCR, various imaging strategies have been reported. For example, a microwell array has been placed on an automatic slide scanning system (Zeiss Axio Imager DIC/Fluorescence Microscope) for a full array imaging (Fig. 5**E**) (Dimov et al., 2014). The exposure was set to cover 70% dynamic range of the CCD (Peltier cooled, Sony ICX 285 sensor). In another study, an inverted fluorescent microscope (Nikon Eclipse Ti-U, Tokyo, Japan) exposing for 3 s at 100-fold magnification has been used for imaging purpose (Zhang et al., 2012). Zhong's group has developed their own microscope (Zhong et al., 2011) with a 20 mW, 488 nm laser source (Cyan; Picarro, Sunnyvale, CA) to visualize the interior of the microfluidic channels. A two band pass filter have discriminated the fluorescence collected through the objective lens: 512/25 nm and 543/22 nm for FAM and VIC fluorophores respectively. The fluorescence has been detected by two H5784-20 photomultipliers and simultaneously recorded at 200 kHz sampling rate with an USB-625 data acquisition card. The droplets have been imaged through the objective lens with backside illumination from a light-emitting diode (LED) (wavelenth: 850 nm). At last, a short-pass filter is applied to separate the optical paths for fluorescence detection and imaging, and a Guppy CCD camera. Besides, imaging of a chip has demonstrated after target amplification using a Maestro Ex IN-VIVO imaging system (CRI Maestro) (Zhu et al., 2014). Fluorescence images have been acquired by a large area CCD system with an enlarged image observed under a fluorescence microscope (OLYMPUS). Fluorescence was been excited at 455 nm and the emitted light was collected by a CCD with a 495 nm long-pass filter.

On the other hand, a lens-free on-chip imaging technique has been introduced, which is composed of a plasmonic chip, an LED, a battery, and a CMOS imager chip for rapid and sensitive detection of nucleic acid (Colle et al., 2013). The resolution of this lens-free on-chip imaging is 25 μm. This lens-free imaging resolution offers a great potential for quantification in dPCR.

Till now, the widely used image processing tools includes ImageJ, Matlab (Dimov et al., 2014; Fan and Quake, 2007; Zhu et al., 2014), LabView (Zhong et al., 2011), and Mathematica (Strain et al., 2013). ImageJ v4.4 (NIH, USA) and MatLAB 5.3 (MathWorks, El Segundo CA, USA) software have been demonstrated in analyzing the images (Fig. 5**F**) (Dimov et al., 2014). A Matlab program also has been developed to process and obtain the chip's fluorescent image after 40 cycles of thermal cycling and which determined the number of fluorescent channel (Fan and Quake, 2007). A custom algorithm in Mathematica has been developed to classify each channel into positive, negative, or ambiguous (Strain et al., 2013). The copy number of template per unit volume has been determined by the ratio of positive reaction observed. Since dPCR provides an endpoint detection, some compartments contain more than one target, thus, Poisson distribution plays an important role at this point (Perkel, 2014) to eliminate outliers. The template number existing in a droplet was assumed to follow the Poisson distribution, meanwhile, the number of positive droplets was assumed to follow a binomial distribution. In another study, an algorithm in LabView has been developed to detect positive droplets as contiguous region above a fixed or manually set intensity threshold (Zhong et al., 2011).

## 5. Biomedical applications of dPCR

The two main applications of dPCR in biomedical fields are rare mutation detection and nucleic acid quantification (Huggett and Whale, 2013). The detection of rare mutants means a specific rare DNA molecule could be detected in the vast background (Vogelstein and Kinzler, 1999). In qPCR, the primers or probes are normally used to detect the wild-type sequences, which may not accurately detect the target of interest in genetic testing. In contrast, dPCR is capable of absolutely quantifying the mutated target genes by using a small amount of sample. For example, the absolute numbers of MON810 transgene and High-Mobility Group (HMG) maize reference gene copies in DNA samples have been determined using dPCR duplex assay without the need for calibration curves, with the detection limit as low as 5 copies of target DNA (Morisset et al., 2013).

Particularly, based on different detection target, dPCR mainly plays an important role in pathogen detection, copy number variation (CNV) detection , MicroRNA (miRNA) expression analysis , next-generation sequencing, single-cell gene expression analysis and chromosome abnormality detection (Fig. 6). Furthermore, rare cancer target detection (Mangolini et al., 2015; Milbury et al., 2014; Parsons et al., 2016; Qin et al., 2016; Schwarzenbach et al., 2011), establishment of accurate reference or standards (Bhat and Emslie, 2016; Corbisier et al., 2015; Dong et al., 2015; Huggett et al., 2015) and genetically modified components identification (Bucher and Köppel, 2015; Findlay et al., 2016; Gerdes et al., 2016; Zhu et al., 2016) are all the crucial and potential applications of dPCR. Recently, the development of this field has been extended towards the detection of tumor DNA in liquid biopsy of tumor patients, with the ability of detecting target DNA even at levels as low as 0.1% of total DNA in the blood (Chi, 2016).

cell populations (Dimov et al., 2014). The fluorescence intensity of the cleaved probes is detected by an automated fluorescence microscope scanner and processed through custom scripts in ImageJ and MatLab. The intensity signals are quantified and normalized from each mRNA amplification. **(F)** The end point fluorescence of the B20pl microwell PCR reaction before and after cycle 40 (Dimov et al., 2014). There is a clear log-linear trend between well intensity and the number of cells per well after amplifying the promoter region of the Nanog gene. It shows that the well intensity is a semi-quantitative indicator of the initial concentration of target DNA. Images reprinted from (Dimov et al., 2014; Pekin et al., 2011; Zhong et al., 2011; Zhu et al., 2015).

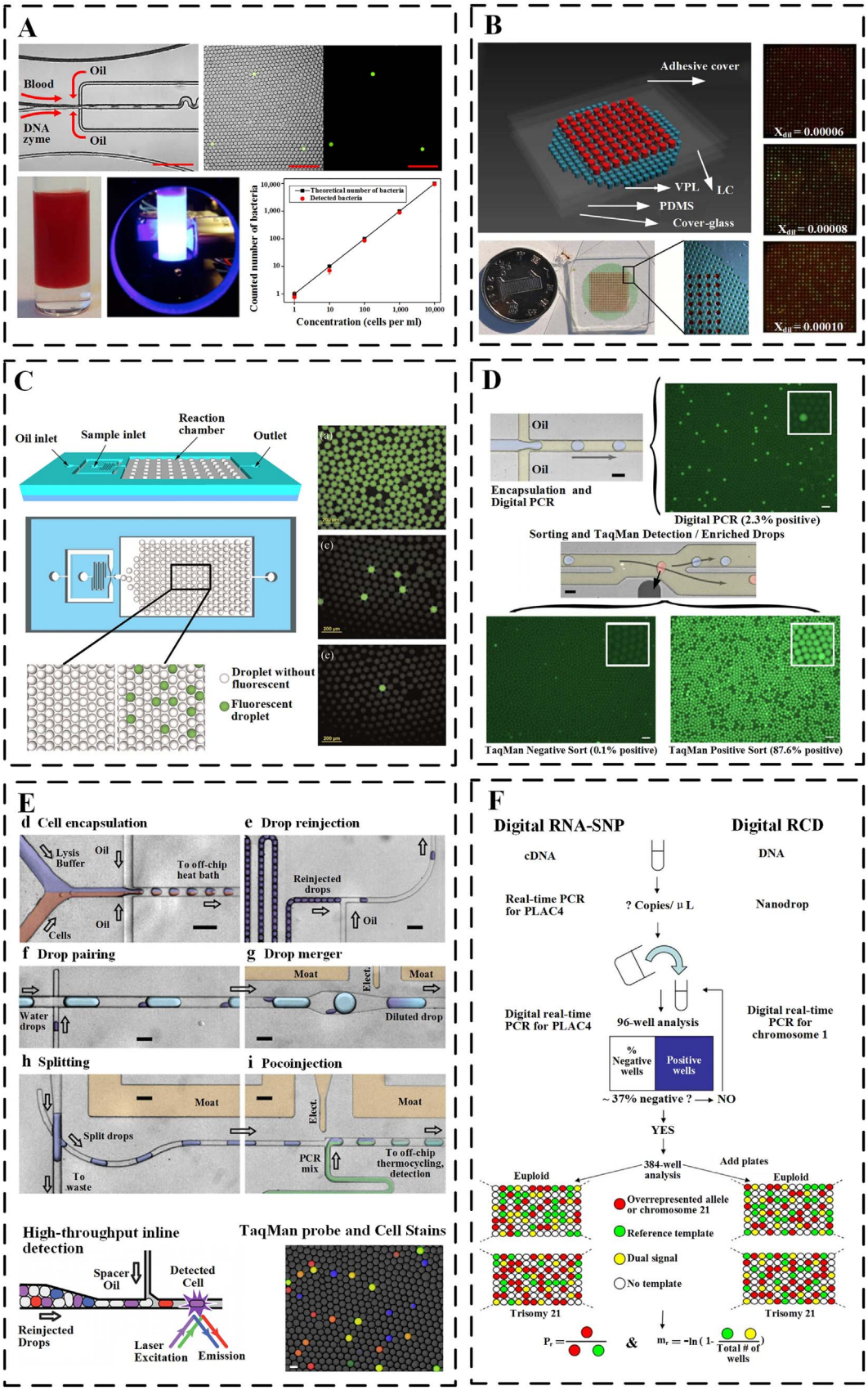


**Fig. 6. Biomedical applications of dPCR. (A)** Pathogen detection: rapid detection of single bacteria in unprocessed blood using integrated comprehensive droplet digital detection (Kang et al., 2014). **(B)** Copy number variation (CNV) detection: a localized temporary negative pressure assisted microfluidic device for detecting keratin 19 in A549 lung carcinoma cells with digital PCR (Tian et al., 2015b). **(C)** MicroRNA (miRNA) expression analysis: absolute quantification of lung cancer related microRNA by droplet digital PCR (Wang et al., 2015). **(D)** Next-generation sequencing result validation: microfluidic droplet enrichment for targeted sequencing (Eastburn et al., 2015). **(E)** Single-cell gene expression analysis: ultrahigh-throughput mammalian single-cell reverse-transcriptase polymerase chain reaction in microfluidic drops (Eastburn et al., 2013). **(F)** Chromosome abnormality detection: digital PCR for the molecular detection of fetal chromosomal aneuploidy (Lo et al., 2007). Images reprinted from (Eastburn et al., 2015, 2013; Kang et al., 2014; Lo et al., 2007; Tian et al., 2015b; Wang et al., 2015).

### 5.1. Pathogen detection

The numerous individual reaction partitions of dPCR makes it possible to study the single cell genomics of pathogens (Gutierrez-Aguirre et al., 2015). A droplet-based system named “IC 3D” has been successfully used to detect single bacteria in raw blood within a few minutes (Fig. 6**A**) (Kang et al., 2014). A microfluidic-based dPCR has also been demonstrated to quantify the presence of pig intestinal bacteria (*Prevotella*) dependent on the specific drug being used (Looft et al., 2014). In addition, dPCR has also been performed to sensitively detect human immunodeficiency virus (HIV) nucleic acid (Kiselinova et al., 2014; Perez-Santiago et al., 2015; Yukl et al., 2013) in cerebrospinal fluid (CSF) cell and peripheral blood mononuclear cell (PBMC) (Oliveira et al., 2015). The housekeeping gene Ribonuclease P protein subunit p30 (RPP30) has been used as a reference for absolute quantification of HIV nucleic acids. It has been reported that 64% of cerebrospinal fluid cell spheres contain HIV-DNA whereas 53% contains HIV-RNA.

In human cytomegalovirus (HCMV) detection, two digital PCR platforms, namely QX100™ droplet digital PCR system (Bio-Rad Laboratories®) and Biomark™ HD system (Fluidigm®) have been used simultaneously for sample testing (Pavsic et al., 2015). When using the QX100 system, the copy number of virus in direct amplification-detection has shown 18% higher than plasma extracted DNA, and 35% higher than PBS solution extracted DNA. As for the detection using the Biomark system, the virus copy numbers has been shown 26% higher than plasma extracted DNA and 53% higher than PBS solution extracted DNA. Overall, in pathogen detection, dPCR have been shown to successfully detect low target concentration in various samples with reliable test results.

### 5.2. Copy number variation (CNV) detection

CNV is an important source of human genetic variation, and is closely associated with a large number of human diseases. Digital PCR enables the detection of copy number variation with the detection limit as low as 1–100 copies (Marx, 2014). Microwell based digital PCR has been used to detect the mitochondrial DNA (mtDNA) copy number in germline karyoplasts (Wang et al., 2014). A correlation between proximal Spinal muscular atrophy (SMA) severity and centromeric Survival of motor neuron 2 (SMN2) gene copy number has been determined using the QuantStudio 3D™ dPCR system (Stabley et al., 2015). In addition, a homemade device called “localized temporary negative pressure assisted microfluidic device” has been demonstrated to quantify the amount of keratin 19 in A549 lung carcinoma cell lines, and a good correlation has been observed between the amount of fluorescent spots and dilution factor (Fig. 6**B**) (Tian et al., 2015b). Similarly, in another lung cancer study, Alexandra (Pender et al., 2015) and Chien (Lin et al., 2015) have successfully detected the copy numbers of mutated KRAS (Kirsten rat sarcoma viral oncogene) gene and EGFR (Epidermal growth factor receptor) gene respectively *via* dPCR. The detection limit of mutated KRAS gene has shown 2000: 1 (a mutated KRAS gene has been detected in two thousand wild KRAS genes), which is much sensitive than that using sanger sequencing (10: 1) and next-generation sequencing (50: 1). In addition to the lung cancer, in detection of HGSOC (high-grade serous ovarian cancer), the numbers of deleted NF1 (Neurofibromin 1) deletion and mutant TP53 p.R175H (Tumor protein 53) have been succesfully quantified in HGSOC tissues (Schwarz et al., 2015). In short, the aforementioned studies are all about the detection of copy number variation of genes or mutation, which have currently attracted significant research interest in the field of dPCR and have become the mainstream of dPCR applications.

### 5.3. MicroRNA (miRNA) expression analysis

In cancer detection, microRNA (Ambros, 2004; Bartel 2004) has been known as a promising circulating biomarker in liquid biopsy for early diagnosis of cancers (Ma et al., 2013; Ono et al., 2015; Zhang et al., 2015). Digital PCR, especially water-in-oil based (or droplet based) dPCR enables absolute quantification of target microRNAs in lung tissue samples (Fig. 6**C**) (Wang et al., 2015). Besides, The microwell based dPCR (Thermo Fisher Scientific®) has been adopted to detect the copy numbers of five kinds of microRNA biomarkers (mir-16-5p, mir-21-5p, mir-126-3p, mir-486-5p and mir-660-5p) in lung cancer detection (Conte et al., 2015). In this work, the plasma, cell lysates and tissue from lung cancer patients have been used for target miRNA extraction. Synthetic oligonucleotide (as internal control) has been used to create a standard curve to evaluate the performance of the assay in terms of efficiency, precision, and sensitivity. In another study, dPCR has been performed to quantify the expression level of two lung cancer-associated miRNAs (miR-31 and miR-210) in lung cancer patients (Li et al., 2014). This technology has also been demonstrated in other cancer research, including diagnosis of microRNAs in the serum of breast cancer patients (Mangolini et al., 2015) and absolute quantification of cell-free microRNAs in cancer patients (Ferracin et al., 2015; Tsukuda et al., 2016).

### 5.4. Next-generation sequencing validation

Unlike conventional qPCR, dPCR allows accurate result quantification (either 0 or 1) independent of varying amplicon lengths, which could potentially generate amplification bias in qPCR (Kim et al., 2011; White et al., 2009). Digital PCR has been reported to provide sensitive and absolute calibration for high throughput sequencing (Robin et al., 2016), as shown by the accurate quantification of 454 and Solexa sequencing libraries (White et al., 2009). This method has successfully reduced the sample volume more than 1000-fold without the step of pre-amplification, minimizing the undesired effects of bias. Additionally , microfluidic droplet enrichment for sequence analysis (MESA), a new target enrichment technology has been introduced. In this work, 250 kb targeted genomic DNA from 5 different genomic loci have been enriched by 31.6-fold using MESA (Fig. 6**D**) (Eastburn et al., 2015). Fragments of genomic DNA are extracted for TaqMan probe based droplet dPCR. The TaqMan positive droplets are recovered by dielectrophoresis, followed by the removal of amplicons by enzymatic reaction prior to sequencing. Taken together, this method enables comprehensive identification of genetic polymorphisms within the targeted loci with requirement for only a small amount of DNA, making it very suitable for the study of genetic variation in biomedical applications.

### 5.5. Single-cell gene expression analysis

In the absence of need for pre-amplification, dPCR allows single-cell gene expression analysis without amplification bias, highlighting its potential to substitute the conventional qPCR (Fig. 6**E**). With this, cell development mechanism could be evaluated in depth. For instance, to study single cell transcriptome, microbeads are modified with barcode primers, each single cell combined with these microbeads is encapsulated in water-in-oil droplets (Klein et al., 2015; Macosko et al., 2015). A self-seeding microwell chip that consists of 6400 microwells has been developed, with a pore of approximately 5 μm at the bottom of each microwell. Once a single cell landed on the pore, it could prevent other cells flow through the microwell, leading the subsequent cells to flow into the next microwell (Swennenhuis et al., 2015). With this method, a large number of single cells could be quickly and efficiently formed in each microwell (Jen et al., 2012a, 2012b; Lindstrom and Andersson-Svahn, 2011; Lindstrom et al., 2009; Yang et al., 2015).

In fact, single-cell restriction analysis of methylation (SCRAM) has

been introduced to analyze methylation level on multiple sites of single cell. SCRAM mainly includes the following steps: isolation and lysis of single cell; digestion of genomic DNA using methylation sensitive restriction enzyme; two cycles of PCR amplification for multiple sites, and determination of methylation status of target (Cheow et al., 2015). Using the droplet based dPCR to analysis single cell's gene expression (Brouzes et al., 2009; Mazutis et al., 2013), about 1 million single-cell hybridomas have been successfully detected within 2–6 h.

Additionally, circulating tumor cell (CTC) (Cohen et al., 2008; Plaks et al., 2013; Williams, 2013) screening and detection (Kim et al., 2016; Stott et al., 2010; Vona et al., 2000; Yang et al., 2015) by dPCR with analysis of single cell gene expression has also been introduced (Pfitzner et al., 2014). Westbrook's group have summarized the micro-nano technologies for generating high throughput single cells and have laid the foundation for using dPCR in single cell gene expression analysis (Weaver et al., 2014). Undoubtedly, this application has attracted much interest of researchers around the world.

### 5.6. Chromosome abnormality detection

To date, chromosome abnormality is possible to be detected by dPCR (Zimmermann et al., 2008). Chromosomal abnormality refers to deletions, additions, or irregular changes of a segment from chromosome (Izatt, 2012). Non-invasive prenatal screening (NIPS) or detection of chromosomal abnormality in fetus by dPCR has been introduced (Fig. 6**F**) (El Khattabi et al., 2016; Lee et al., 2015; Lo et al., 2007; Perlado et al., 2016; Xu et al., 2016b). Further, chimaerism in hematopoiesis has also been accurately quantified by dPCR (Stahl et al., 2015). A drop-phase method combined with water-in-oil based dPCR had been applied to ascertain the phase of DNA sequence variants, without cloning or dilution of sample to single molecule (Regan et al., 2015). It is worth mentioning that by performing dPCR, tedious gene cloning and manual dilution of sample are not required, lengthy and complicated operation steps could also be addressed at the same time.

## 6. Conclusion and future perspective

In conclusion, dPCR represents a novel, sensitive, accurate and multiplex quantification strategy to detect a scarce amount of target nucleic acid in complex clinical sample. Various sample dispersion methods for dPCR, including droplet based, micowell based-capillary force driving, channel based and printing based sample dispersion have been introduced to address the tedious dilution step required in conventional dPCR. The proper employment of these sample dispersion methods offers hundreds to millions of nanoliter or even picoliter-scale reaction partitions, enabling sensitive and accurate absolute quantification of multiplex target nucleic acids.

The integration of portable thermal cycling amplification (Ahrberg et al., 2016b) or isothermal amplification (Rodriguez-Manzano et al., 2016) into dPCR platform, coupling with on-chip fluorescent dots image processing (Devadhasan et al., 2015) or fluorescent signal counting, particularly in microfluidic-based dPCR allows absolute nucleic acids detection under many circumstances. This kind of integrated dPCR platform would offers great potential in wide range of applications including early diagnosis and prognosis monitoring.

However, dPCR with unique accuracy, small reaction volume and high sensitivity is still subject to a number of challenges for further development (Brenan and Morrison, 2005): (I) How to perform simple, robust and efficient droplets manipulation on microplate or microfluidic chip to set up PCR systems for single molecule detection without the aid of external instruments? (II) Realize good isolation of microreaction systems in PCR thermal cycling and droplets manipulation process; (III) Considering the requirements of molecular diagnostic in POCT, how can we miniaturize the dPCR system without affecting data quality and detection speed, simultaneously. An self-priming compartmentalization (SPC) based microfluidic chip has been fabricated to perform digital loop-mediated amplification (digital LAMP) (Zhu et al., 2012), and the digital droplet multiple displacement amplification (ddMDA) also has been applied for whole genome sequencing in a trace of DNA sample (Rhee et al., 2016; Xu et al., 2016a). These digital-isothermal amplification methods are power-free, valve-free, inexpensive and labor time saving. So, cheap and readily available material, simple fabrication process, and energy-efficient amplification assay would greatly reduce the cost, and complexity of dPCR system. (IV) With the existing and emerging dispersion strategies of dPCR, what orders of sensitivity can we reach to, when we analyzing a limited DNA sample with an unknown concentration. But the prediction is that dPCR's detection limit will continuously improve with the increasing number of partitions benefiting from rapid development of micro-nano machining technology.

Although there exist a numbers of commercial dPCR systems based on different partition technology, most of them are expensive with poor integration and multiplexing capability (Baker, 2012; Day et al., 2013). Besides dPCR, there are also other biosensors that are not based on PCR, but use molecular beacons, enzymatic, immunological, and other biorecognition or biomimetic techniques in DNA and RNA recognition (Hepel et al., 2012; Stobiecka and Chalupa, 2016; Stobiecka and Chałupa, 2015; Stobiecka et al., 2007). These biosensors are simple, rapid, and low cost, which hold great potential for DNA and RNA recognition. With the rapid development of microfluidic technology and microfabrication, we envision that dPCR system could be continuously improved without adding cost and greatly simplified without compromising its performance. If some burgeoning auxiliary detection technique such as isothermal amplification (Zhao et al., 2015) and lens-free imaging (Takehara et al., 2016) could be integrated in dPCR, the dPCR system will be fully minimized for various biomedical applications in the near future, especially in developing world.

## Acknowledgments

This work was financially supported by the Major International Joint Research Program of China (11120101002), International Science & Technology Cooperation Program of China (2013DFG02930), and National Instrumentation Program (No. 2013YQ190467).

## References

Ahrberg, C.D., Manz, A., Neuzil, P., 2016b. Anal. Chem. 88, 4803–4807.
Ahrberg, C.D., Ilic, B.R., Manz, A., Neuzil, P., 2016a. Lab Chip 16, 586–592.
Allen, D., Butt, A., Cahill, D., Wheeler, M., Popert, R., Swaminathan, R., 2004. Ann. N.Y. Acad. Sci. 1022, 76–80.
Ambros, V., 2004. Nature 431, 350–355.
Arrabito, G., Galati, C., Castellano, S., Pignataro, B., 2013. Lab Chip 13, 68–72.
Baker, M., 2012. Nat. Methods 9, 541–544.
Ball, P., 2013. Nature 496, 419–420.
Barrett, A.N., Chitty, L.S., 2014. Developing noninvasive diagnosis for single-gene disorders: the role of digital PCR. In: Biassoni, R., Raso, A. (Eds.), Quantitative Real-Time PCR: Methods and Protocols. Springer, New York, NY, 215–228.
Bartel, D.P., 2004. Cell 116, 281–297.
Bartlett, J.M., Stirling, D., 2003. A short history of the polymerase chain reaction. In: Bartlett, J.M.S., Stirling, D. (Eds.), PCR Protocols. Humana Press, Totowa, NJ, 3–6.
Bartsch, M.S., Edwards, H.S., Lee, D., Moseley, C.E., Tew, K.E., Renzi, R.F., Van de Vreugde, J.L., Kim, H., Knight, D.L., Sinha, A., 2015. PloS One 10, e0118182.
Beer, N.R., Hindson, B.J., Wheeler, E.K., Hall, S.B., Rose, K.A., Kennedy, I.M., Colston, B.W., 2007. Anal. Chem. 79, 8471–8475.
Belmonte, F.R., Martin, J.L., Frescura, K., Damas, J., Pereira, F., Tarnopolsky, M.A., Kaufman, B.A., 2016. Sci. Rep. 6, 25186.
Bhat, S., McLaughlin, J.L., Emslie, K.R., 2011. Analyst 136, 724–732.
Bhat, S., Emslie, K.R., 2016. Biomol. Detect Quantif.
Bio-Rad, 2013. QX200™ Droplet Generator Instruction Manual. < http://www.bio-rad.com/en-us/product/qx200-droplet-digital-pcr-system > . (accessed 23.02.14).
Blow, N., 2007. Nat. Methods 4, 869–875.
Blow, N., 2009. Nat. Methods 6, 683.
Brenan, C., Morrison, T., 2005. Drug Discov. Today: Technol. 2, 247–253.
Brouzes, E., Medkova, M., Savenelli, N., Marran, D., Twardowski, M., Hutchison, J.B., Rothberg, J.M., Link, D.R., Perrimon, N., Samuels, M.L., 2009. Proc. Natl. Acad. Sci.

USA 106, 14195–14200.
Bucher, T.B., Köppel, R., 2015. Eur. Food Res. Technol. 242, 927–934.
Burns, M., Burrell, A., Foy, C., 2010. Eur. Food Res. Technol. 231, 353–362.
Chapela, M.-J., Garrido-Maestu, A., Cabado, A.G., 2015. Cogent Food Agric. 1, 1013771.
Chapman, S.J., Hill, A.V., 2012. Nat. Rev. Genet. 13, 175–188.
Chen, W.W., Balaj, L., Liau, L.M., Samuels, M.L., Kotsopoulos, S.K., Maguire, C.A., Loguidice, L., Soto, H., Garrett, M., Zhu, L.D., Sivaraman, S., Chen, C., Wong, E.T., Carter, B.S., Hochberg, F.H., Breakefield, X.O., Skog, J., 2013. Mol. Ther. Nucleic Acids 2, e109.
Cheow, L.F., Quake, S.R., Burkholder, W.F., Messerschmidt, D.M., 2015. Nat. Protoc. 10, 619–631.
Chi, K.R., 2016. Nature 532, 269–271.
Churchill, M.J., Deeks, S.G., Margolis, D.M., Siliciano, R.F., Swanstrom, R., 2016. Nat. Rev. Microbiol. 14, 55–60.
Cohen, S.J., Punt, C.J., Iannotti, N., Saidman, B.H., Sabbath, K.D., Gabrail, N.Y., Picus, J., Morse, M., Mitchell, E., Miller, M.C., Doyle, G.V., Tissing, H., Terstappen, L.W., Meropol, N.J., 2008. Am. J. Clin. Oncol. 26, 3213–3221.
Colle, F., Vercruysse, D., Peeters, S., Liu, C., Stakenborg, T., Lagae, L., Del-Favero, J., 2013. Lab Chip 13, 4257–4262.
Conte, D., Verri, C., Borzi, C., Suatoni, P., Pastorino, U., Sozzi, G., Fortunato, O., 2015. BMC Genom. 16, 1–11.
Corbisier, P., Pinheiro, L., Mazoua, S., Kortekaas, A.M., Chung, P.Y., Gerganova, T., Roebben, G., Emons, H., Emslie, K., 2015. Anal. Bioanal. Chem. 407, 1831–1840.
Dangla, R., Kayi, S.C., Baroud, C.N., 2013. Proc. Natl. Acad. Sci. USA 110, 853–858.
Day, E., Dear, P.H., McCaughan, F., 2013. Methods 59, 101–107.
Debski, P.R., Gewartowski, K., Sulima, M., Kaminski, T.S., Garstecki, P., 2015. Anal. Chem. 87, 8203–8209.
Deeks, S.G., Autran, B., Berkhout, B., Benkirane, M., Cairns, S., Chomont, N., Chun, T.W., Churchill, M., Di Mascio, M., Katlama, C., Lafeuillade, A., Landay, A., Lederman, M., Lewin, S.R., Maldarelli, F., Margolis, D., Markowitz, M., Martinez-Picado, J., Mullins, J.I., Mellors, J., Moreno, S., O'Doherty, U., Palmer, S., Penicaud, M.C., Peterlin, M., Poli, G., Routy, J.P., Rouzioux, C., Silvestri, G., Stevenson, M., Telenti, A., Van Lint, C., Verdin, E., Woolfrey, A., Zaia, J., Barre-Sinoussi, F., 2012. Nat. Rev. Immunol. 12, 607–614.
deMello, A.J., 2006. Nature 442, 394–402.
Devadhasan, J.P., Yoo, I.S., Kim, S., 2015. Curr. Appl. Phys. 15, 402–411.
Dimov, I.K., Lu, R., Lee, E.P., Seita, J., Sahoo, D., Park, S.M., Weissman, I.L., Lee, L.P., 2014. Nat. Commun. 5, 3451.
Dong, L., Meng, Y., Sui, Z., Wang, J., Wu, L., Fu, B., 2015. Sci. Rep. 5, 13174.
Eastburn, D.J., Sciambi, A., Abate, A.R., 2013. Anal. Chem. 85, 8016–8021.
Eastburn, D.J., Huang, Y., Pellegrino, M., Sciambi, A., Ptacek, L.J., Abate, A.R., 2015. Nucleic Acids Res. 43, e86.
El Khattabi, L.A., Rouillac-Le Sciellour, C., Le Tessier, D., Luscan, A., Coustier, A., Porcher, R., Bhouri, R., Nectoux, J., Serazin, V., Quibel, T., Mandelbrot, L., Tsatsaris, V., Vialard, F., Dupont, J.M., 2016. PLoS One 11, e0155009.
El-Ali, J., Perch-Nielsen, I.R., Poulsen, C.R., Bang, D.D., Telleman, P., Wolff, A., 2004. Sens. Actuators A: Phys. 110, 3–10.
Fan, H.C., Quake, S.R., 2007. Anal. Chem. 79, 7576–7579.
Ferracin, M., Lupini, L., Salamon, I., Saccenti, E., Zanzi, M., Rocchi, A., Da Ros, L., Zagatti, B., Musa, G., Bassi, C., 2015. Oncotarget 6, 14545–14555.
Findlay, S.D., Vincent, K.M., Berman, J.R., Postovit, L.M., 2016. PLoS One 11, e0153901 .
Floren, C., Wiedemann, I., Brenig, B., Schütz, E., Beck, J., 2015. Food Chem. 173, 1054–1058.
Friend, J., Yeo, L.Y., 2011. Rev. Mod. Phys. 83, 647.
Gerdes, L., Iwobi, A., Busch, U., Pecoraro, S., 2016. Biomol. Detect Quantif. 7, 9–20.
Guan, W., Chen, L., Rane, T.D., Wang, T.H., 2015. Sci. Rep. 5, 13795.
Gutierrez-Aguirre, I., Racki, N., Dreo, T., Ravnikar, M., 2015. Droplet digital PCR for absolute quantification of pathogens. In: Lacomme, C. (Ed.), Plant Pathology: Techniques and Protocols. Springer, New York, NY, 331–347.
Guttenberg, Z., Muller, H., Habermuller, H., Geisbauer, A., Pipper, J., Felbel, J., Kielpinski, M., Scriba, J., Wixforth, A., 2005. Lab Chip 5, 308–317.
Hepel, M., Stobiecka, M., Peachey, J., Miller, J., 2012. Mutat. Res. 735, 1–11.
Heyries, K.A., Tropini, C., VanInsberghe, M., Doolin, C., Petriv, O.I., Singhal, A., Leung, K., Hughesman, C.B., Hansen, C.L., 2011. Nat. Methods 8, 649–651.
Hindson, B.J., Ness, K.D., Masquelier, D.A., Belgrader, P., Heredia, N.J., Makarewicz, A.J., Bright, I.J., Lucero, M.Y., Hiddessen, A.L., Legler, T.C., Kitano, T.K., Hodel, M.R., Petersen, J.F., Wyatt, P.W., Steenblock, E.R., Shah, P.H., Bousse, L.J., Troup, C.B., Mellen, J.C., Wittmann, D.K., Erndt, N.G., Cauley, T.H., Koehler, R.T., So, A.P., Dube, S., Rose, K.A., Montesclaros, L., Wang, S., Stumbo, D.P., Hodges, S.P., Romine, S., Milanovich, F.P., White, H.E., Regan, J.F., Karlin-Neumann, G.A., Hindson, C.M., Saxonov, S., Colston, B.W., 2011. Anal. Chem. 83, 8604–8610.
Hindson, C.M., Chevillet, J.R., Briggs, H.A., Gallichotte, E.N., Ruf, I.K., Hindson, B.J., Vessella, R.L., Tewari, M., 2013. Nat. Methods 10, 1003–1005.
Hofer, U., 2016. Nat. Rev. Microbiol. 14, 120.
Hoffmann, J., Hin, S., Stetten, Fv, Zengerle, R., Roth, G., 2012. RSC Adv. 2, 3885–3889.
Houssin, T., Cramer, J., Grojsman, R., Bellahsene, L., Colas, G., Moulet, H., Minnella, W., Pannetier, C., Leberre, M., Plecis, A., Chen, Y., 2016. Lab Chip.
Hudecova, I., 2015. Clin. Biochem 48, 948–956.
Huggett, J.F., Whale, A., 2013. Clin. Chem. 59, 1691–1693.
Huggett, J.F., Cowen, S., Foy, C.A., 2015. Clin. Chem. 61, 79–88.
Huggett, J.F., Foy, C.A., Benes, V., Emslie, K., Garson, J.A., Haynes, R., Hellemans, J., Kubista, M., Mueller, R.D., Nolan, T., Pfaffl, M.W., Shipley, G.L., Vandesompele, J., Wittwer, C.T., Bustin, S.A., 2013. Clin. Chem. 59, 892–902.
Issadore, D., Humphry, K.J., Brown, K.A., Sandberg, L., Weitz, D.A., Westervelt, R.M., 2009. Lab Chip 9, 1701–1706.
Izatt, L., 2012. Clin. Med. 12, (297-297).
Jaque, D., Maestro, L.M., Del Rosal, B., Haro-Gonzalez, P., Benayas, A., Plaza, J., Rodríguez, E.M., Solé, J.G., 2014. Nanoscale 6, 9494–9530.
Jen, C.P., Hsiao, J.H., Maslov, N.A., 2012b. Sensors 12, 347–358.
Jen, C.P., Amstislavskaya, T.G., Liu, Y.H., Hsiao, J.H., Chen, Y.H., 2012a. Sensors 12, 6967–6977.
Jung, J.H., Choi, S.J., Park, B.H., Choi, Y.K., Seo, T.S., 2012. Lab chip 12, 1598–1600.
Kang, D.K., Ali, M.M., Zhang, K., Huang, S.S., Peterson, E., Digman, M.A., Gratton, E., Zhao, W., 2014. Nat. Commun. 5, 5427.
Kang, Q., Parkin, B., Giraldez, M.D., Tewari, M., 2016. BioTechniques 60, 175.
Kanwal, R., Gupta, S., 2012. Clin. Genet. 81, 303–311.
Kathiresan, S., Srivastava, D., 2012. Cell 148, 1242–1257.
Kim, H., Vishniakou, S., Faris, G.W., 2009. Lab Chip 9, 1230–1235.
Kim, H., Bartsch, M.S., Renzi, R.F., He, J., Van de Vreugde, J.L., Claudnic, M.R., Patel, K.D., 2011. J. Lab Autom. 16, 405–414.
Kim, J., Cho, H., Han, S.I., Han, K.H., 2016. Anal. Chem. 88, 4857–4863.
Kiselinova, M., Pasternak, A.O., De Spiegelaere, W., Vogelaers, D., Berkhout, B., Vandekerckhove, L., 2014. PLoS One 9, e85999.
Kiss, M.M., Ortoleva-Donnelly, L., Beer, N.R., Warner, J., Bailey, C.G., Colston, B.W., Rothberg, J.M., Link, D.R., Leamon, J.H., 2008. Anal. Chem. 80, 8975–8981.
Klein, A.M., Mazutis, L., Akartuna, I., Tallapragada, N., Veres, A., Li, V., Peshkin, L., Weitz, D.A., Kirschner, M.W., 2015. Cell 161, 1187–1201.
Kleppe, K., Ohtsuka, E., Kleppe, R., Molineux, I., Khorana, H., 1971. J. Mol. Biol. 56, 341–361.
Knierim, E., Lucke, B., Schwarz, J.M., Schuelke, M., Seelow, D., 2011. PloS One 6, e28240.
Kondoh, J., Shimizu, N., Matsui, Y., Sugimoto, M., Shiokawa, S., 2009. Sens. Actuators A: Phys. 149, 292–297.
Konstantinidis, K., Kitsis, R.N., 2012. Nature 485, 179–180.
Kopp, M.U., De Mello, A.J., Manz, A., 1998. Science 280, 1046–1048.
Köppel, R., Bucher, T., 2015. Eur. Food Res. Technol. 241, 427–439.
Kreutz, J.E., Munson, T., Huynh, T., Shen, F., Du, W., Ismagilov, R.F., 2011. Anal. Chem. 83, 8158–8168.
Laig, M., Ho, B., Majumdar, N.S., Lac, L.T., Chan, F., Sathiyaa, R., Russel, I., Cifuentes, P., Straub, T., Varma, K., 2015. Cancer Res. 75, (5251-5251).
Lalani, S.R., Shaw, C., Wang, X., Patel, A., Patterson, L.W., Kolodziejska, K., Szafranski, P., Ou, Z., Tian, Q., Kang, S.H., Jinnah, A., Ali, S., Malik, A., Hixson, P., Potocki, L., Lupski, J.R., Stankiewicz, P., Bacino, C.A., Dawson, B., Beaudet, A.L., Boricha, F.M., Whittaker, R., Li, C., Ware, S.M., Cheung, S.W., Penny, D.J., Jefferies, J.L., Belmont, J.W., 2013. Eur. J. Hum. Genet. 21, 173–181.
Lee, S.Y., Shim, S.H., Youn, J.-P., Kim, S.J., Kim, J.H., Jung, S.A., Choi, H.J., Oh, M.J., Lee, K.-R., Cha, D.H., Hwang, S.Y., 2015. BioChip J. 9, 339–352.
Leng, X., Zhang, W., Wang, C., Cui, L., Yang, C.J., 2010. Lab Chip 10, 2841–2843.
Li, B., Fan, J., Li, J., Chu, J., Pan, T., 2015. Biomicrofluidics 9, 054101.
Li, L., Sui, Z.-W., Wang, J., Zang, C., Yu, X.-B., 2012. Prog. Biochem. Biophys. 39, 1017–1023.
Li, N., Ma, J., Guarnera, M.A., Fang, H., Cai, L., Jiang, F., 2014. J. Cancer Res. Clin. Oncol. 140, 145–150.
Liao, C.-S., Lee, G.-B., Liu, H.-S., Hsieh, T.-M., Luo, C.-H., 2005. Nucleic Acids Res. 33, (e156-e156).
Lievens, A., Jacchia, S., Kagkli, D., Savini, C., Querci, M., 2016. PLoS One 11, e0153317.
Lin, C.C., Huang, W.L., Wei, F., Su, W.C., Wong, D.T., 2015. Expert Rev. Mol. Diagn. 15, 1427–1440.
Lindstrom, S., Andersson-Svahn, H., 2011. Biochim. Biophys. Acta 1810, 308–316.
Lindstrom, S., Eriksson, M., Vazin, T., Sandberg, J., Lundeberg, J., Frisen, J., Andersson-Svahn, H., 2009. PLoS One 4, e6997.
Link, D., Anna, S.L., Weitz, D., Stone, H., 2004. Phys. Rev. Lett. 92, 054503.
Lo, Y.M.D., Lun, F.M.F., Chan, K.C.A., Tsui, N.B.Y., Chong, K.C., Lau, T.K., Leung, T.Y., Zee, B.C.Y., Cantor, C.R., Chiu, R.W.K., 2007. Copyr. (2007) Natl. Acad. Sci. USA 104, 13116–13121.
Looft, T., Allen, H.K., Casey, T.A., Alt, D.P., Stanton, T.B., 2014. Front. Microbiol. 5, 276.
Ma, J., Li, N., Guarnera, M., Jiang, F., 2013. Biomark. Insights 8, 127–136.
Macosko, E.Z., Basu, A., Satija, R., Nemesh, J., Shekhar, K., Goldman, M., Tirosh, I., Bialas, A.R., Kamitaki, N., Martersteck, E.M., 2015. Cell 161, 1202–1214.
de Magalhaes, J.P., 2013. Nat. Rev. Cancer 13, 357–365.
Majumdar, N., Wessel, T., Marks, J., 2015. PLoS One 10, e0118833.
Mangolini, A., Ferracin, M., Zanzi, M.V., Saccenti, E., Ebnaof, S.O., Poma, V.V., Sanz, J.M., Passaro, A., Pedriali, M., Frassoldati, A., Querzoli, P., Sabbioni, S., Carcoforo, P., Hollingsworth, A., Negrini, M., 2015. Biomark. Res. 3, 1–9.
Marcheggiani, S., Spurio, R., Cimarelli, L., Tito, D., Mancini, L., 2015. Int. J. Environ. Res Public Health 12, 15400–15408.
Marx, V., 2014. Nat. Methods 11, 241–245.
Mazutis, L., Gilbert, J., Ung, W.L., Weitz, D.A., Griffiths, A.D., Heyman, J.A., 2013. Nat. Protoc. 8, 870–891.
Mazutis, L., Baret, J.C., Treacy, P., Skhiri, Y., Araghi, A.F., Ryckelynck, M., Taly, V., Griffiths, A.D., 2009. Lab Chip 9, 2902–2908.
McCaughan, F., Dear, P.H., 2010. J. Pathol. 220, 297–306.
Milbury, C.A., Zhong, Q., Lin, J., Williams, M., Olson, J., Link, D.R., Hutchison, B., 2014. Biomol. Detect Quantif. 1, 8–22.
Miralles, V., Huerre, A., Malloggi, F., Jullien, M.-C., 2013. Diagnostics 3, 33–67.
Mogi, K., Sugii, Y., Yamamoto, T., Fujii, T., 2014. Sens Actuators B 201, 407–412.
Morisset, D., Stebih, D., Milavec, M., Gruden, K., Zel, J., 2013. PLoS One 8, e62583.
Mujahid, A., Iqbal, N., Afzal, A., 2013. Biotechnol. Adv. 31, 1435–1447.
Neuzil, P., Pipper, J., Hsieh, T.M., 2006. Mol. Biosyst. 2, 292–298.
Neuzil, P., Novak, L., Pipper, J., Lee, S., Ng, L.F., Zhang, C., 2010. Lab Chip 10, 2632–2634.

Nie, Z., Seo, M., Xu, S., Lewis, P.C., Mok, M., Kumacheva, E., Whitesides, G.M., Garstecki, P., Stone, H.A., 2008. Microfluid Nanofluid 5, 585–594.
Nisisako, T., Torii, T., Higuchi, T., 2002. Lab Chip 2, 24–26.
Nixon, G., Garson, J.A., Grant, P., Nastouli, E., Foy, C.A., Huggett, J.F., 2014. Anal. Chem. 86, 4387–4394.
Oliveira, M.F., Gianella, S., Letendre, S., Scheffler, K., Kosakovsky Pond, S.L., Smith, D.M., Strain, M., Ellis, R.J., 2015. PLoS One 10, e0139510.
Ono, S., Lam, S., Nagahara, M., Hoon, D., 2015. J. Clin. Med. 4, 1890–1907.
Ottesen, E.A., Hong, J.W., Quake, S.R., Leadbetter, J.R., 2006. Science 314, 1464–1467.
Parsons, H.A., Beaver, J.A., Park, B.H., 2016. Circulating plasma tumor DNA. In: Stearns, V. (Ed.), Novel Biomarkers in the Continuum of Breast Cancer. Springer International Publishing, Cham, 259–276.
Pavsic, J., Zel, J., Milavec, M., 2015. Anal. Bioanal. Chem. 408, 67–75.
Pekin, D., Skhiri, Y., Baret, J.C., Le Corre, D., Mazutis, L., Salem, C.B., Millot, F., El Harrak, A., Hutchison, J.B., Larson, J.W., Link, D.R., Laurent-Puig, P., Griffiths, A.D., Taly, V., 2011. Lab Chip 11, 2156–2166.
Pender, A., Garcia-Murillas, I., Rana, S., Cutts, R.J., Kelly, G., Fenwick, K., Kozarewa, I., Gonzalez de Castro, D., Bhosle, J., O'Brien, M., Turner, N.C., Popat, S., Downward, J., 2015. PLoS One 10, e0139074.
Perez-Santiago, J., Schrier, R.D., de Oliveira, M.F., Gianella, S., Var, S.R., Day, T.R., Ramirez-Gaona, M., Suben, J.D., Murrell, B., Massanella, M., Cherner, M., Smith, D.M., Ellis, R.J., Letendre, S.L., Mehta, S.R., 2015. J. NeuroVirol. 22, 191–200.
Perkel, J.M., 2014. Science 344, 212–214.
Perlado, S., Bustamante-Aragones, A., Donas, M., Lorda-Sanchez, I., Plaza, J., Rodriguez de Alba, M., 2016. PLoS One 11, e0153258.
Pfitzner, C., Schroder, I., Scheungraber, C., Dogan, A., Runnebaum, I.B., Durst, M., Hafner, N., 2014. Sci. Rep. 4, 3970.
Plaks, V., Koopman, C.D., Werb, Z., 2013. Science 341, 1186–1188.
Poser, S., Schulz, T., Dillner, U., Baier, V., Köhler, J.M., Schimkat, D., Mayer, G., Siebert, A., 1997. Sens. Actuators A: Phys. 62, 672–675.
Psaltis, D., Quake, S.R., Yang, C., 2006. Nature 442, 381–386.
Qi, Z., Ma, Y., Deng, L., Wu, H., Zhou, G., Kajiyama, T., Kambara, H., 2011. Analyst 136, 2252–2259.
Qin, D., Xia, Y., Whitesides, G.M., 2010. Nat. Protoc. 5, 491–502.
Qin, Z., Ljubimov, V.A., Zhou, C., Tong, Y., Liang, J., 2016. Chin. J. Cancer 35, 36.
Ramakrishnan, R., Qin, J., Jones, R.C., Weaver, L.S., 2013. Integrated fluidic circuits (IFCs) for digital PCR. In: Jenkins, G., Mansfield, D.C. (Eds.), Microfluidic Diagnostics: Methods and Protocols. Humana Press, Totowa, NJ, 423–431.
Reboud, J., Bourquin, Y., Wilson, R., Pall, G.S., Jiwaji, M., Pitt, A.R., Graham, A., Waters, A.P., Cooper, J.M., 2012. Proc. Natl. Acad. Sci. USA 109, 15162–15167.
Regan, J.F., Kamitaki, N., Legler, T., Cooper, S., Klitgord, N., Karlin-Neumann, G., Wong, C., Hodges, S., Koehler, R., Tzonev, S., McCarroll, S.A., 2015. PLoS One 10, e0118270.
Rhee, M., Light, Y.K., Meagher, R.J., Singh, A.K., 2016. PLoS One 11, e0153699.
Robin, J.D., Ludlow, A.T., LaRanger, R., Wright, W.E., Shay, J.W., 2016. Sci. Rep. 6, 24067.
Roche, P.J., Beitel, L.K., Khan, R., Lumbroso, R., Najih, M., Cheung, M.C.-K., Thiemann, J., Veerasubramanian, V., Trifiro, M., Chodavarapu, V.P., 2012. Analyst 137, 4475–4481.
Rodriguez-Manzano, J., Karymov, M.A., Begolo, S., Selck, D.A., Zhukov, D.V., Jue, E., Ismagilov, R.F., 2016. ACS Nano 10, 3102–3113.
Rose, D., 2000. Microfluidic technologies and instrumentation for printing DNA microarrays. In: Schena, M. (Ed.), Microarray Biochip Technology. Eaton Publishing, Natick, MA, 19–38.
Ruijter, J.M., Ramakers, C., Hoogaars, W.M., Karlen, Y., Bakker, O., van den Hoff, M.J., Moorman, A.F., 2009. Nucleic Acids Res. 37, e45.
Sackmann, E.K., Fulton, A.L., Beebe, D.J., 2014. Nature 507, 181–189.
Saiki, R.K., Scharf, S., Faloona, F., Mullis, K.B., Horn, G.T., Erlich, H.A., Arnheim, N., 1985. Science 230, 1350–1354.
Sakakihara, S., Araki, S., Iino, R., Noji, H., 2010. Lab Chip 10, 3355–3362.
Schmittgen, T.D., Livak, K.J., 2008. Nat. Protoc. 3, 1101–1108.
Schneider, T., Kreutz, J., Chiu, D.T., 2013. Anal. Chem. 85, 3476–3482.
Schwarz, R.F., Ng, C.K., Cooke, S.L., Newman, S., Temple, J., Piskorz, A.M., Gale, D., Sayal, K., Murtaza, M., Baldwin, P.J., Rosenfeld, N., Earl, H.M., Sala, E., Jimenez-Linan, M., Parkinson, C.A., Markowetz, F., Brenton, J.D., 2015. PLoS Med. 12, e1001789.
Schwarzenbach, H., Hoon, D.S., Pantel, K., 2011. Nat. Rev. Cancer 11, 426–437.
Schwarzenbach, H., Stoehlmacher, J., Pantel, K., Goekkurt, E., 2008. Ann. N.Y. Acad. Sci. 1137, 190–196.
Sefrioui, D., Sarafan-Vasseur, N., Beaussire, L., Baretti, M., Gangloff, A., Blanchard, F., Clatot, F., Sabourin, J.C., Sesboue, R., Frebourg, T., Michel, P., Di Fiore, F., 2015. Dig. Liver Dis. 47, 884–890.
Shembekar, N., Chaipan, C., Utharala, R., Merten, C.A., 2016. Lab Chip 16, 1314–1331.
Shen, F., Du, W., Kreutz, J.E., Fok, A., Ismagilov, R.F., 2010b. Lab Chip 10, 2666–2672.
Shen, F., Du, W., Davydova, E.K., Karymov, M.A., Pandey, J., Ismagilov, R.F., 2010a. Anal. Chem. 82, 4606–4612.
Shen, F., Sun, B., Kreutz, J.E., Davydova, E.K., Du, W., Reddy, P.L., Joseph, L.J., Ismagilov, R.F., 2011. J. Am. Chem. Soc. 133, 17705–17712.
Shilton, R.J., Mattoli, V., Travagliati, M., Agostini, M., Desii, A., Beltram, F., Cecchini, M., 2015. Adv. Funct. Mater. 25, 5895–5901.
Son, J.H., Cho, B., Hong, S., Lee, S.H., Hoxha, O., Haack, A.J., Lee, L.P., 2015. Light.: Sci. Appl. 4, e280.
Song, Q., Gao, Y., Zhu, Q., Tian, Q., Yu, B., Song, B., Xu, Y., Yuan, M., Ma, C., Jin, W., Zhang, T., Mu, Y., Jin, Q., 2015. Biomed. Microdev. 17, 1–8.
Stabley, D.L., Harris, A.W., Holbrook, J., Chubbs, N.J., Lozo, K.W., Crawford, T.O., Swoboda, K.J., Funanage, V.L., Wang, W., Mackenzie, W., Scavina, M., Sol-Church, K., Butchbach, M.E., 2015. Mol. Genet. Genom. Med 3, 248–257.
Stahl, T., Bohme, M.U., Kroger, N., Fehse, B., 2015. Exp. Hematol. 43, 462–468, (e461).
Stears, R.L., Martinsky, T., Schena, M., 2003. Nat. Med. 9, 140–145.
Stobiecka, M., Chałupa, A., 2015. Chem. Pap. 69, 62–76.
Stobiecka, M., Chalupa, A., 2016. J. Phys. Chem. B 120, 4782–4790.
Stobiecka, M., Cieśla, J.M., Janowska, B., Tudek, B., Radecka, H., 2007. Sensors 7, 1462–1479.
Stott, S.L., Hsu, C.H., Tsukrov, D.I., Yu, M., Miyamoto, D.T., Waltman, B.A., Rothenberg, S.M., Shah, A.M., Smas, M.E., Korir, G.K., Floyd, F.P., Jr., Gilman, A.J., Lord, J.B., Winokur, D., Springer, S., Irimia, D., Nagrath, S., Sequist, L.V., Lee, R.J., Isselbacher, K.J., Maheswaran, S., Haber, D.A., Toner, M., 2010. Proc. Natl. Acad. Sci. USA 107, 18392–18397.
Strain, M.C., Lada, S.M., Luong, T., Rought, S.E., Gianella, S., Terry, V.H., Spina, C.A., Woelk, C.H., Richman, D.D., 2013. PLoS One 8, e55943.
Streets, A.M., Huang, Y., 2014. Curr. Opin. Biotechnol. 25, 69–77.
Sun, Y., Zhou, X., Yu, Y., 2014. Lab Chip 14, 3603–3610.
Susiarjo, M., Bartolomei, M.S., 2014. Science 345, 733–734.
Svobodova, I., Pazourkova, E., Horinek, A., Novotna, M., Calda, P., Korabecna, M., 2015. PLoS One 10, e0142572.
Swennenhuis, J.F., Tibbe, A.G., Stevens, M., Katika, M.R., van Dalum, J., Duy Tong, H., van Rijn, C.J., Terstappen, L.W., 2015. Lab Chip 15, 3039–3046.
Tadmor, A.D., Ottesen, E.A., Leadbetter, J.R., Phillips, R., 2011. Science 333, 58–62.
Takehara, H., Nagasaki, M., Sasagawa, K., Takehara, H., Noda, T., Tokuda, T., Ohta, J., 2016. Jpn. J. Appl. Phys. 55, (03DF03).
Tanaka, H., Yamamoto, S., Nakamura, A., Nakashoji, Y., Okura, N., Nakamoto, N., Tsukagoshi, K., Hashimoto, M., 2015. Anal. Chem. 87, 4134–4143.
Tay, A., Kulkarni, R.P., Karimi, A., Di Carlo, D., 2015. Lab Chip 15, 4379–4382.
Taylor, S.C., Carbonneau, J., Shelton, D.N., Boivin, G., 2015. J. Virol. Methods 224, 58–66.
Teh, S.Y., Lin, R., Hung, L.H., Lee, A.P., 2008. Lab Chip 8, 198–220.
Tellinghuisen, J., Spiess, A.N., 2015a. Anal. Chem. 87, 1889–1895.
Tellinghuisen, J., Spiess, A.N., 2015b. Anal. Chem. 87, 8925–8931.
ThermoFisher, 2015. QuantStudio™ 3D Digital PCR System User Guide. ⟨http://www.thermofisher.com/cn/zh/home/life-science/pcr/digital-pcr/quantstudio-3d-digital-pcr-system.html⟩. (accessed 13.10.15).
Tian, Q., Yu, B., Mu, Y., Xu, Y., Ma, C., Zhang, T., Jin, W., Jin, Q., 2015a. RSC Adv. 5, 81889–81896.
Tian, Q.C., Song, Q., Xu, Y.N., Zhu, Q.Y., Yu, B.W., Jin, W., Jin, Q.H., Mu, Y., 2015b. Anal. Methods 7, 2006–2011.
Trypsteen, W., Vynck, M., De Neve, J., Bonczkowski, P., Kiselinova, M., Malatinkova, E., Vervisch, K., Thas, O., Vandekerckhove, L., De Spiegelaere, W., 2015. Anal. Bioanal. Chem. 407, 5827–5834.
Tsukuda, M., Wiederkehr, R.S., Cai, Q., Majeed, B., Fiorini, P., Stakenborg, T., Matsuno, T., 2016. Jpn. J. Appl. Phys. 55, (04EM05).
Unger, M.A., Chou, H.P., Thorsen, T., Scherer, A., Quake, S.R., 2000. Science 288, 113–116.
Velve-Casquillas, G., Le Berre, M., Piel, M., Tran, P.T., 2010. Nano Today 5, 28–47.
Vogelstein, B., Kinzler, K.W., 1999. Proc. Natl. Acad. Sci. USA 96, 9236–9241.
Vogelstein, B., Papadopoulos, N., Velculescu, V.E., Zhou, S., Diaz, L.A., Jr., Kinzler, K.W., 2013. Science 339, 1546–1558.
Vona, G., Sabile, A., Louha, M., Sitruk, V., Romana, S., Schütze, K., Capron, F., Franco, D., Pazzagli, M., Vekemans, M., Lacour, B., Bréchot, C., Paterlini-Bréchot, P., 2000. Am. J. Pathol. 156, 57–63.
Wang, P., Jing, F., Li, G., Wu, Z., Cheng, Z., Zhang, J., Zhang, H., Jia, C., Jin, Q., Mao, H., Zhao, J., 2015. Biosens. Bioelectron. 74, 836–842.
Wang, T., Sha, H., Ji, D., Zhang, H.L., Chen, D., Cao, Y., Zhu, J., 2014. Cell 157, 1591–1604.
Weaver, W.M., Tseng, P., Kunze, A., Masaeli, M., Chung, A.J., Dudani, J.S., Kittur, H., Kulkarni, R.P., Di Carlo, D., 2014. Curr. Opin. Biotechnol. 25, 114–123.
Whale, A.S., Huggett, J.F., Cowen, S., Speirs, V., Shaw, J., Ellison, S., Foy, C.A., Scott, D.J., 2012. Nucleic Acids Res. 40, e82.
White, A.K., Heyries, K.A., Doolin, C., VanInsberghe, M., Hansen, C.L., 2013. Anal. Chem. 85, 7182–7190.
White, R.A., 3rd, Blainey, P.C., Fan, H.C., Quake, S.R., 2009. BMC Genom. 10, 1–12.
Whitesides, G.M., Ostuni, E., Takayama, S., Jiang, X., Ingber, D.E., 2001. Annu. Rev. Biomed. Eng. 3, 335–373.
Williams, R., Peisajovich, S.G., Miller, O.J., Magdassi, S., Tawfik, D.S., Griffiths, A.D., 2006. Nat. Methods 3, 545–550.
Williams, S.C., 2013. Proc. Natl. Acad. Sci. USA 110, 4861.
Witters, D., Knez, K., Ceyssens, F., Puers, R., Lammertyn, J., 2013. Lab Chip 13, 2047–2054.
Witters, D., Sun, B., Begolo, S., Rodriguez-Manzano, J., Robles, W., Ismagilov, R.F., 2014. Lab Chip 14, 3225–3232.
Wu, Y.L., Dahlhoff, V., He, L., Chen, C.F., 2014. Cancer Res. 74, (5241-5241).
Xu, P., Zheng, X., Tao, Y., Du, W., 2016a. Anal. Chem. 88, 3171–3177.
Xu, S., Zou, B., Xiang, Z., Miao, M., Song, Q., Huang, H., Wu, H., Zhou, G., 2016b. Anal. Methods 8, 2138–2143.
Yager, P., Edwards, T., Fu, E., Helton, K., Nelson, K., Tam, M.R., Weigl, B.H., 2006. Nature 442, 412–418.
Yang, Y., Rho, H.S., Stevens, M., Tibbe, A.G., Gardeniers, H., Terstappen, L.W., 2015. Lab Chip 15, 4331–4337.
Yoon, D.S., Lee, Y.-S., Lee, Y., Cho, H.J., Sung, S.W., Oh, K.W., Cha, J., Lim, G., 2002. J. Micromech. Microeng. 12, 813.
Yukl, S.A., Boritz, E., Busch, M., Bentsen, C., Chun, T.W., Douek, D., Eisele, E., Haase, A., Ho, Y.C., Hutter, G., Justement, J.S., Keating, S., Lee, T.H., Li, P., Murray, D., Palmer, S., Pilcher, C., Pillai, S., Price, R.W., Rothenberger, M., Schacker, T.,

Siliciano, J., Siliciano, R., Sinclair, E., Strain, M., Wong, J., Richman, D., Deeks, S.G., 2013. PLoS Pathog. 9, e1003347.
Zhang, C., Xing, D., 2010. Chem. Rev. 110, 4910–4947.
Zhang, K., Kang, D.K., Ali, M.M., Liu, L., Labanieh, L., Lu, M., Riazifar, H., Nguyen, T.N., Zell, J.A., Digman, M.A., Gratton, E., Li, J., Zhao, W., 2015. Lab Chip 15, 4217–4226.
Zhang, W.Y., Zhang, W., Liu, Z., Li, C., Zhu, Z., Yang, C.J., 2012. Anal. Chem. 84, 350–355.
Zhang, Y., Zhu, Y., Yao, B., Fang, Q., 2011. Lab Chip 11, 1545–1549.
Zhao, Y., Chen, F., Li, Q., Wang, L., Fan, C., 2015. Chem. Rev. 115, 12491–12545.
Zhong, Q., Bhattacharya, S., Kotsopoulos, S., Olson, J., Taly, V., Griffiths, A.D., Link, D.R., Larson, J.W., 2011. Lab Chip 11, 2167–2174.
Zhu, P., Wang, C., Huang, K., Luo, Y., Xu, W., 2016. Int. J. Mol. Sci. 17, 402.
Zhu, Q., Qiu, L., Yu, B., Xu, Y., Gao, Y., Pan, T., Tian, Q., Song, Q., Jin, W., Jin, Q., Mu, Y., 2014. Lab Chip 14, 1176–1185.
Zhu, Q.Y., Gao, Y.B., Yu, B.W., Ren, H., Qiu, L., Han, S.H., Jin, W., Jin, Q.H., Mu, Y., 2012. Lab Chip 12, 4755–4763.
Zhu, Y., Zhang, Y.X., Liu, W.W., Ma, Y., Fang, Q., Yao, B., 2015. Sci. Rep. 5, 9551.
Zimmermann, B.G., Grill, S., Holzgreve, W., Zhong, X.Y., Jackson, L.G., Hahn, S., 2008. Prenat. Diagn. 28, 1087–1093.